*Palaeontologia Electronica*
palaeo-electronica.org

# Lower Jurassic corals from Morocco with skeletal structures convergent with those of Paleozoic rugosan corals

**Raphaël Vasseur, Simon Boivin, Bernard Lathuilière, Iuliana Lazar, Christophe Durlet, Rowan-Clare Martindale, Stéphane Bodin, and Khalid Elhmidi**

## ABSTRACT

*Neorylstonia* nom. nov. *pseudocolumellata,* a replacement name for *Mesophyllum pseudocolumellatum* Beauvais, 1986, is only known from uppermost Sinemurian to uppermost Pliensbachian (Lower Jurassic) strata of Morocco. This solitary coral species went extinct during the Pliensbachian-Toarcian transition (~183.5 My), which is currently considered to be a second order biodiversity crisis linked to a period of rapid and global paleoenvironmental disturbances. *Neorylstonia pseudocolumellata* has a distinctive skeletal organization. The axial structure of the corallite, which has no equivalent in Mesozoic taxa, is reminiscent of the skeletal organization of some Paleozoic rugose corals such as *Amygdalophyllum* Dun and Benson, 1920, or *Rylstonia* Hudson and Platt, 1927. This similarity is based on the occurrence of a calicular boss also named pseudocolumella. As Rugosa and Scleractinia do not appear closely related, we consider that this feature cannot be due to evolutionary inheritance from a Rugosan ancestor. The morphological aspects of the skeleton have been assessed in order to understand the function and growth of this axial "calicular boss" as well as to more precisely describe the genus and species characters. The organization of the septal apparatus points to a typical Scleractinian pattern, which is also supported by the original aragonitic mineralogy of the skeleton. This implies a convergence phenomenon, leaving open the question of the functional significance of such a calicular organization. We posit that this feature was used for sexual reproduction and so did not always develop in a population.

Raphaël Vasseur. Université de Lorraine, CNRS, lab. GeoRessources, UMR 7359, BP 70239, 54506, Vandoeuvre-lès-Nancy Cedex, France. raphael.vasseur@univ-lorraine.fr
Simon Boivin. University of Geneva, Department of Earth Sciences, Rue des Maraîchers 13, 1205 Geneva, Switzerland. simon.boivin@unige.ch

**http://zoobank.org/14F3D176-317B-4AFF-B165-5CD5CD1220F9**

Vasseur, Raphaël, Boivin, Simon, Lathuilière, Bernard, Lazar, Iuliana, Durlet, Christophe, Martindale, Rowan-Clare, Bodin, Stéphane, and Elhmidi, Khalid. 2019. Lower Jurassic corals from Morocco with skeletal structures convergent with those of Paleozoic rugosan corals. *Palaeontologia Electronica* 22.2.48A 1-32. https://doi.org/10.26879/874
palaeo-electronica.org/content/2019/2654-neorylstonia-paper

Copyright: August 2019 Paleontological Society.
This is an open access article distributed under the terms of Attribution-NonCommercial-ShareAlike 4.0 International (CC BY-NC-SA 4.0), which permits users to copy and redistribute the material in any medium or format, provided it is not used for commercial purposes and the original author and source are credited, with indications if any changes are made.
creativecommons.org/licenses/by-nc-sa/4.0/

Bernard Lathuilière. Université de Lorraine, CNRS, lab. GeoRessources, UMR 7359, BP 70239, 54506, Vandoeuvre-lès-Nancy Cedex, France. bernard.lathuiliere@univ-lorraine.fr
Iuliana Lazar. University of Bucharest, Faculty of Geology and Geophysics, Department of Geology and Paleontology, 1, N. Balcescu Ave., RO – 010041, Bucharest, Romania. iuliana.lazar@g.unibuc.ro
Christophe Durlet. UMR CNRS 6282 Biogéosciences, Univ. Bourgogne Franche-Comté, 21000 Dijon, France. christophe.durlet@u-bourgogne.fr
Rowan-Clare Martindale. Department of Geological Sciences, Jackson School of Geosciences, University of Texas at Austin, 2275 Speedway Stop C9000, Austin, Texas 78712, USA. martindale@jsg.utexas.edu
Stéphane Bodin. Aarhus University, Department of Geoscience, Høegh-Guldbergs Gade 2, 8000 Aarhus C, Denmark. stephane.bodin@geo.au.dk
Khalid Elhmidi. Département de l'Energie et des Mines Direction de la Géologie, Rue Abou Marouane Essaadi BP 6208, Haut Agdal, Rabat, Morocco. k.elhmidi@mem.gov.ma

Keywords: Corals; Early Jurassic; CT scan; taxonomy; Rugosa; Scleractinia; new name

Submission: 3 April 2018. Acceptance: 2 July 2019.

## INTRODUCTION

The Pliensbachian/Toarcian boundary event (~183.5 Ma) and the Toarcian Oceanic Anoxic Event (Early Toarcian, ~183 Ma) are two intervals of worldwide environmental and ecological disruption during the Early Jurassic. This period is known for large-scale black shale deposits (e.g., Jenkyns , 1985, 1988; Jenkyns and Clayton, 1986; Schmid-Röhl et al., 2002) and multiple negative excursions of δ13C affecting exogenic carbon reservoirs and associated sediments (e.g., Pálfy et al., 2002; Littler et al., 2010; Bodin et al., 2016). These events have been associated with marine eutrophication, increased ocean anoxia (e.g., Röhl et al., 2001; Morard et al., 2003, Bodin et al., 2010), high global temperatures (e.g., Vakhrameyev, 1982; Jenkyns, 2003; Rosales et al., 2004, Suan et al., 2010), putative acidification of the oceans (Trecalli et al., 2012), and global disturbances of the carbon cycle attributed to the pulsed emplacement of the Karoo-Ferrar flood basalts (Duncan et al., 1997; Sell et al., 2014; Burgess et al., 2015). These paleoenvironmental disturbances appear to be contemporaneous with a second-order biodiversity crisis affecting various taxonomic groups such as ammonites, foraminifera, bivalves, and brachiopods (e.g., Raup and Sepkoski, 1984, 1986; Harries and Little, 1999; Caswell et al., 2009; Dera et al., 2010; Guex et al., 2012; Goričan et al., 2013; Caruthers et al., 2013; Danise et al., 2013, 2015; Caruthers et al., 2014; Martindale and Aberhan, 2017). Nevertheless, data about coral turnover are relatively sparse, and the only detailed study is based on a compilation of bibliographical data (Lathuilière and Marchal, 2009).

This publication focuses on one of the victims of the Pliensbachian/Toarcian boundary crisis; this unique coral has features that are reminiscent of Paleozoic coral structures, likely a case of convergent evolution rather than inheritance. As Rugosa and Scleractinia are not closely related, a case of inheritance is excluded (see for examples Oliver, 1980; Fedorowski, 1997). This taxon was initially described in Beauvais (1986) as *Mesophyllum pseudocolumellatum* but the genus name is currently unavailable because of homonymy; thus a nomen novum is required. The original description of this species was established on the basis of a narrow sampling of only seven poorly preserved specimens from Beni Tadjit in Morocco (Menchikoff collections), and the genus is based on these seven samples and six other specimens from the Jebel Bou Dahar found in the Du Dresnay collections. These other samples were considered by Beauvais as another potential species, but the preservation was too poor to validate this assumption. The present study is based on the analysis of 91 specimens of *Mesophyllum* collected and/or pictured by our team during field campaigns from the Dades Valley and the Amellagou region in the Central High Atlas as well as from the Guigou Plateau in the Middle Atlas of Morocco. This significant new sampling effort results in new insights about the morphology of this taxon, its taxonomy, its biostratigraphic attribution, and sedimentological context. This work also raises new questions about the phylogeny and function morphology of this coral taxon.

## GEOLOGICAL SETTING

In Morocco, studied sites are located in the Amellagou area, the Dades Valley, and the Guigou

Plateau; GPS locations are presented in Table 1. Liassic distal environments in Morocco contain abundant biostratigraphically useful ammonites (see synthesis in Dommergues and Meister, 2017) and so there is a relatively good biostratigraphical framework established for the coral occurrences reported here.

The Guigou Plateau is located in Middle Atlas (Figure 1.1, 1.2), where several huge carbonate buildups from Carixian (lower Pliensbachian substage) to Domerian (upper Pliensbachian substage) shape the landscape. This carbonate platform is generally interpreted as capping a tilted block limited in the southeast by the "Northern Middle-Atlasic Accident" (Colo, 1961; El Arabi et al., 1987), which marks the boundary between tabular Middle-Atlas and "folded" Middle-Atlas, and by the "Tizi n'Trettène accident" in the northwest, which separates two distinct plateaus of the Tabular Middle Atlas. One of the sampling areas has been concentrated especially on one of these bioconstructions: the Koudiat Ech Chehem. It is an approximately 100 m high buildup prograding towards the southwest and rising above limestone-marls deposits including early Domerian ammonites *Protogrammoceras* (Morabet, 1974 according to El Arabi et al., 1987). Marly limestone and marl alternations containing *Hildaites gyralis*, *Hildaites subserpentinus*, and *Harpoceras* cf. *madagascariense* (all known from the Serpentinum Zone, early Toarcian) onlap the flanks of the bioconstruction. The other outcrop for sampling is part of the "Tailil-out" section located in the western part of the Guigou Plateau, directly west from Koudiat Ech Chehem. This outcrop corresponds to lower or middle Carixian stage; it is topped by a level that stratigraphically corresponds to the Maftah 2 Formation (comforted by personal communications from André Charrière in the field), which contains the middle Carixian ammonite *Tropidoceras* (see Charrière et al., 2011, p. 62). The outcrop level sampled corresponds to the transition between the Maftah 1 and Maftah 2 formations. In fact, the core of Maftah 1 Formation shows mudstone to packstone limestone alternations containing bivalves, foraminifera, and algae, sometimes with cross-bedding. Then, the top of Maftah 1 Formation is made of cross-bedded oolitic and bioclastic calcarenites including corals in some beds. A major discontinuity showing a ferruginous hardground, including wood, marks the top of this Formation. The Maftah 2 Formation includes more silicified

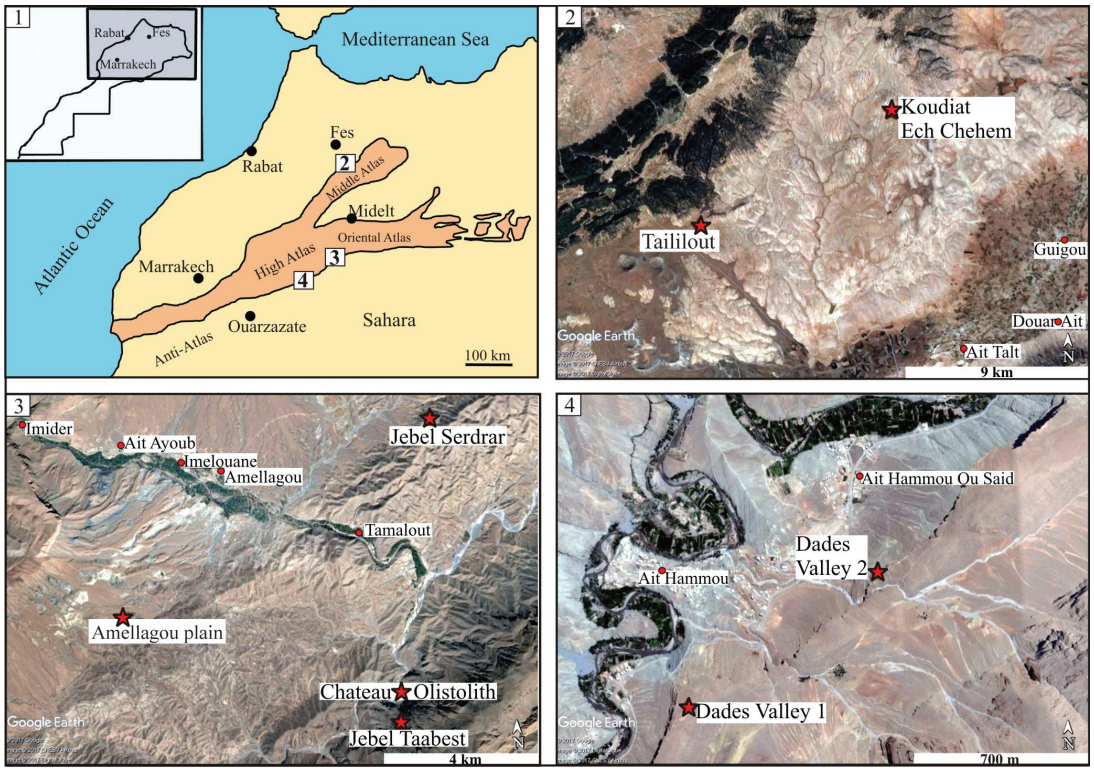


**FIGURE 1.** Geographic location of the different sampling sites where *N. pseudocolumellata* has been found in Morocco. **1,** General location of the studied areas in the Atlas Mountains (orange zone); **2,** Guigou plateau; **3,** Amellagou municipality; **4,** Dades Valley.

bioclastic and oolitic limestones or thin argillaceous limestones and is dated by the presence of middle Carixian ammonite *Tropidoceras* at the base and the upper Carixian ammonites *Becheiceras gallicum* and *Fuciniceras* aff. *bastianii* (Davoei zone) in the core of the member. The subsequent Maftah 3 Formation records deeper depositional environments with clay and limestones alternations including lower to middle Domerian ammonites.

The municipality of Amellagou is in the southern part of the Central High Atlas rift basin, in the Gueris Valley (Figure 1.1, 1.3). Some of the samples have been found in Pliensbachian-aged (from Ibex to Spinatum ammonite chronozones) coral and sponge bioherms, which grew on the upper slope that bordered the thick southern carbonate platform. Abundant lithiotid communities developed on subtidal lagoon paleoenvironments on this platform, outcropping at the top of Jebel Taabest, for example. Numerous other specimens have been collected in olistoliths that slipped eastwards and northwards, up to the lower slope, in a hemipelagic environment. These olistoliths are associated with slumps and calciturbidites, related to synsedimentary faults and tilting; they are attributed to the lateral transition between the Choucht and Ouchbis Formations. Olistoliths show a boundstone to floatstone texture, with solitary and colonial corals, sponges, gastropods, serpulid worms, crinoids, brachiopods, echinoids tests and spines, and occasional chaetetid sponges and microbialites. Some of the olistoliths also contain lithiotid bivalves (including *Cochlearites* and *Opisoma* genera). Numerous olistoliths originating from the carbonate platform slipped towards the basin during the latest Pliensbachian lowstand (Spinatum chronozone), just before the drowning of the Taabest platform, which occurred during the earliest Toarcian. Older specimens of presently studied corals have been collected from the Serdrar reef, a 200 m high basinal patch reef. The Serdrar reef is located on a local high, the foot wall of the Serdrar fault, which was tectonically active during the Early Jurassic (Sarih, 2008; Lachkar et al., 2009). Ammonites of the uppermost Sinemurian (Raricostatum chronozone) have been found on the distal slope deposits of this big pinnacle (see Table 1).

The Dades Valley also belongs to the southern margin of the central High Atlas rift basin (Figure 1.1, 1.4). Specimens come from the upper part of the Choucht Formation, which is a proximal equivalent of the Ouchbis Formation. This interval is dated by ammonite biostratigraphy and corresponds to the late Pliensbachian Emaciatum ammonite chronozone, more specifically the Elisa sub-chronozone (Ettaki et al., 2000). The age is confirmed by the presence of the nannofossil *Lotharingius sigillatus* (a marker for the nannofossil subzone NJT5b) found below the Choucht Formation in the Tizguin section (Mattioli et al., 2013; Bodin et al., 2016). The Choucht Formation is a succession of shallow-water deposits made of packstone to mudstone beds deposited in a carbonate platform environment, including phaceloid coral reefs with rare lithiotids bivalves. Nonetheless, ammonites, belemnites and *Zoophycos* ichnofossils are observed in this formation, in close association with the reefs, suggesting relatively deep (shoreface to offshore transition) depositional conditions for this formation (wave influence sedimentary structures have not been observed to date). Despite a thorough investigation of Toarcian outcrops from these regions, no *N. pseudocolumellata* was found in post-Pliensbachian strata, to date.

## MATERIALS AND METHODS

### Materials

The studied material is represented by 77 specimens collected by our team in the Lower Jurassic of Morocco although 14 additional specimens considered in this study come from the collection of the Muséum National d'Histoire Naturelle (MNHN) in Paris, including the holotype of the type species of the genus *Mesophyllum* Beauvais non Schlüter. Four specimens come from the Beni Tadjit (Menchikoff collections), and the others were in the collections of the Museum, associated with a note from Alloiteau but without any locality (they are suspected to come from Morocco, possibly specimens from Menchikoff collections and Du Dresnay collections cited by Beauvais, 1986).

### Terminology: The Concept of Pseudocolumella

The samples correspond to scleractinian solitary corals with an axial structure corresponding to the definition of a pseudocolumella according to Milne-Edwards and Haime (1848) and later Berkowski and Weyer (2012). This term was introduced initially by Milne-Edwards and Haime (1848), as an alternative to the term columella, in view to describe different types of axial structures for skeleton-bearing corals (Rugosa, Scleractinia and Tabulata). The distinction was mainly based on the genesis of the axial edifice: septal origin in the case of pseudocolumella, non-septal origin in the case of a "columella propria" (Berkowski and

**TABLE 1.** Stratigraphic position, coordinates, and sedimentary context of the different sampling sites.

| Sampling sites | Formation | Coordinates | Stage, chronozones | Main biostratigraphic markers (ammonites when not precised) | Depositional environments |
|---|---|---|---|---|---|
| Jebel Serdrar | Aberdouz | N 32.0077<br>W 4.9453 | Upper Sinemurian Oxynotum and Raricostatum chronozones | *Microderoceras (Eteoderoceras)* sp.<br>*Paltechioceras* sp.<br>*Bouhamidoceras ziziense*<br>*Parasteroceras* sp. | A 200m-high coral patch-reef growing on a fault bounded high (or margin), which was tectonically active during the Early Jurassic, surrounded by micritic limestones and marls deposited in lower offshore environment. |
| Jebel Taabest | Choucht to Agoudim | Several in situ patch reefs and slided reefs between N 31.9351 W 4.9594 and N 31.9334 W 5.0020 | Lower Pliensbachian, Jamesoni and Ibex chronozones | Several ammonite taxa such as:<br>*Fuciniceras (Fuciniceras) mellahense-peyrei*<br>*Fuciniceras (Fuciniceras) volubile-pantanelli*<br>*Galaticeras aegoroides*<br>*Metaderoceras* sp. | *Neorylstonia* specimens were observed and collected in both in situ and slided patch reefs, along the slope of the southern carbonate platform. |
| Taililout | Maftah 1 top to Maftah 2 base | N 33.458576<br>W 4.990422 | Lower Pliensbachian, mainly Ibex chronozone (middle Carixian) | A few hundred meters away at the same horizon, corals are associated side by side with:<br>*Tropidoceras* sp.<br>*Liparoceras (Becheiceras) gallicum*<br>*Fuciniceras (Fuciniceras)* aff. *bastianii*<br>And below levels of the Davoei chronozone<br>(Charrière et al. 2011) | Cross bedded oolitic and bioclastic calcarenites including in situ corals, separated by minor discontinuities as bioturbated grounds. A major discontinuity with ferrugineous crusts and wood debris caps the coral-rich facies and corresponds to a deepening during Maftah 1 to Maftah 2 transition. |
| Koudiat Ech Chehem | Maftah 3 | N 33.452816<br>W 4.922526 | Upper Pliensbachian (Domerian) | Below the bioconstruction:<br>*Protogrammoceras celebratum* (Lower Domerian). | Giant bioherm made of interlayered boundstones (pillarstones and mixstones) and crinoidal grainstones and packstones. Environment in the optimal reef window, at the boundary between shoreface and offshore. Well-lit and diverse communities. |
| Dades Valley 1 | Choucht | N 31.5612<br>W 5.9033 | Upper Pliensbachian Spinatum chronozone, mainly Elisa sub-chronozone | Corals associated laterally with:<br>Ammonites: *Emaciaticeras* sp.<br>Nanofossils: *Lotharingius sigillatus*<br>Indicative of a latest Pliensbachian age | Shallow-water deposits made of pack-to-mudstone beds deposited in a carbonate platform environment (shoreface - offshore transition). Reworked algae, ammonites, belemnites and *Zoophycos*. |
| Dades Valley 2 | Choucht | N 31.5683<br>W 5.8935 | | | |
| Amellagou plain | Agoudim | Several olistoliths between N 31.9796 W5.0125 and N31.9555 W5.0388 | Upper Pliensbachian Spinatum chronozone | Coral-rich olistoliths are embedded in hemipelagic marls and limestones with numerous ammonite taxa such as:<br>*Fuciniceras* sp., *Leptaleoceras* sp., *Calliphilloceras* sp., *Leptaleoceras* sp., *Zaghouanites* sp., *Neolioceras* sp., *Emaciaticeras* sp., *Emaciaticeras* gr. *fervidum*, *Emaciaticeras* gr. *emaciatum*, *Canavaria* sp. | *Neorylstonia* specimens were collected from olistoliths resedimented within offshore marls. These olistoliths originated from the shelf break and the upper slope of the southern carbonate platform. |

Weyer, 2012). Even if the distinction was used by some authors (see for example Fedorowski, 1974) the term pseudocolumella has often been forgotten and the term columella applied to describe all skeletal axial structures in corals fossils, especially in the case of scleractinian description. Chevalier (1987) describes the columella of Scleractinia as a part of the skeleton occupying the axial part of the corallites. In this definition, the columella can have a septal origin or a non-septal origin. We choose to reintroduce here the terminology of Milne-Edwards and Haime (1848) for scleractinian corals because the columellae of septal origin described up until now was structurally distinct from the skeletal structure of the specimens described in this study. In fact, columellae of septal origin in scleractinians occur in the following ways: i) in a single lamellae in the main plan of the corallite (lamellar columella); ii) in the projection of septal trabeculae in the axis of the corallite (papillose and spongy columella); iii) in a thickening and welding of the inner edges of septa ("fausse columelle"—fake columella—in Chevalier, 1987). The axial structure described in this study is made of many septal lamellae separated from the main part of septa early in the coral's ontogeny and organized in bilateral symmetry. These features correspond to the description of the axial structure of the example used by Milne-Edwards and Haime (1848): the genus *Clisiophyllum* Dana, 1846 (Berkowski and Weyer, 2012 proposed *Clisiophyllum keyserlingi* M'Coy, 1849 as the definitive morpho-terminological type of the term pseudocolumella). It also corresponds to the description of some pseudocolumella morphologies described by Fedorowski (1974) for the genus *Lophophyllidium* Grabau, 1928. Consequently, we propose that the term pseudocolumella be used for the singular cases of scleractinian corals showing a rugose-like axial structure made of several septal lamellae organized in a bilateral symmetry.

## Methods

The samples have been prepared and analyzed using photographs, polished sections, thin sections, and computed tomography (CT) scans. The usual qualitative observations on polished surfaces and thin sections have been supplemented by morphometric measurements. Nine characters were measured on photographs by the lead author using the measurement software Canvas 9 (see Table 2); these characters are: great calicular diameter (Gd): the longest linear length passing across the center of the calice; small calicular diameter (Sd): the shortest linear length passing across the center of the calice; number of calicular septa (Ns): septa counted along the corallite periphery; homogeneous septal density (hsd): in order to compare all samples with a homogeneous parameter, the septal density of only S1 and S2 (first and second septal size orders) has been measured over a 5 mm distance at the periphery of the calice; length of S1 (lS1): measurement of the longest and the shortest septa of the first size order S1; length of S2 (lS2): measurement of the longest and the shortest S2; length of S3 (lS3): measurement of the longest and the shortest S3; greater pseudocolumella diameter (dp): the longest linear length passing across the center of the calice from the edges of the pseudocolumella in transverse section; number of pseudocolumellar septa (nps): septa counted along the pseudocolumella periphery.

Using these measurements as a basis, four types of transformed data have been produced for the statistical analysis—extrapolated number of calicular septa (exns): the total number of calicular septa has been estimated including hidden or broken septa. In fact, the preservation of samples is often poor, and it is frequently hard to determine if the third order of septa is present; in some cases these septa are partially or completely obscured by stereome thickening deposits or recrystallization. Middle of variation range value for length of S1 (mlS1): middle of variation range value of septa length is obtained by adding the highest and the lowest measured value of septal length for one order and then calculating the average of this sum. Middle of variation range value for length of S2 (mlS2). Middle of variation range value for length of S3 (mlS3).

Finally, two other pieces of information have been added to the database. Sampling outcrop (Os)—some numbers have been allocated to different sampling zones for each sample: 1, Amellagou plain; 2, MNHN; 3, Dades Valley; 4, Jebel Taabest; 5, Beni Tadjit (Menchikoff collection); 6, Jebel Serdrar; 7, Koudiat Ech Chehem; 8, Taililout. Pseudocolumella shape (ps): the two main shapes of pseudocolumella observed have been labelled with associated numbers and each sample has been associated with an apparent pseudocolumella shape. Examples of pseudocolumella observed in transverse section among the samples are presented in Appendix 1.

Measurements have been used to perform univariate and multivariate statistical analysis, in order to distinguish characters and identify poten-

**TABLE 2.** Values of biometrical measurements for each specimen and character considered in this study. Gd = Great calicular diameter; Sd = Small calicular diameter; Ns = Number of septa; exns = extrapolated number of septa; hsd = homogeneous septal density; lS1 = variation range of S1 length; mls1 = middle of the variation range of S1 length value; lS2 = variation range of S2 length; mls2 = middle of the variation range of S2 length value; lS3 = variation range of S3 length; mls3 = middle of the variation range of S3 length value; ps = pseudocolumella shape; pd = great pseudocolumellar diameter; nps = number of pseudocolumellar septa.

| 1 | Sample name | Outcrop number | Gd | Sd | Ns | exns | hsd | lS1 | mlS1 |
|---|---|---|---|---|---|---|---|---|---|
| 2 | AM16177 | 1 | 17.88 | 16.51 | 44 for 1/2 calice | 88 | 5.5 | n.c. | n.c. |
| 3 | A57331-1 | 2 | 23 | 21.9 | 96 | 96 | 4 | 4.15-5.09 | 4.62 |
| 4 | AM16160 | 1 | 18.82 | 18.04 | 44 | 88 | 5.5 | 4.46-5.12 | 4.79 |
| 5 | AM16164 | 1 | 21.37 | 21.29 | 56 | 92 | 4.5 | 4.81-5.15 | 4.98 |
| 6 | AM16164 bis | 1 | 18.9 | 17.95 | 48 | 96 | 5 | 3.56-4.25 | 3.91 |
| 7 | DA2905E1.1 | 3 | 26.28 | 25.8 | 92 | 92 | 4 | 6.61-7.32 | 6.97 |
| 8 | 2703A6 | 1 | 26.8 | 22.7 | 67 | n.c. | 4 | n.c. | n.c. |
| 9 | AM16172 | 4 | 25.07 | 23.7 | 98 | 98 | 4 | 6.14-7.08 | 6.61 |
| 10 | AM16161 | 1 | 18.74 | 18.02 | 48 | 96 | 5 | 4.14-4.31 | 4.23 |
| 11 | A30500-1 | 5 | 21.3 | 19.45 | n.c. | n.c. | n.c. | n.c. | n.c. |
| 12 | A30500-2 | 5 | 18.5 | 17.5 | n.c. | n.c. | n.c. | n.c. | n.c. |
| 13 | A30500-3 | 5 | 14.5 | 14.4 | n.c. | n.c. | n.c. | n.c. | n.c. |
| 14 | A30500-4 | 5 | 18.3 | 18.2 | n.c. | n.c. | n.c. | n.c. | n.c. |
| 15 | AM16175 | 4 | 18.93 | 15.16 | 22 for 1/2 calice | 86 | 4.5 | 3.84-4.45 | 4.15 |
| 16 | A57331-2 | 2 | 22.51 | 21.53 | 48 | 96 | 4 | n.c. | n.c. |
| 17 | A57331-4 | 2 | 16.68 | 16 | 48 S1 + S2 | 96 | 6 | n.c. | n.c. |
| 18 | A57331-5 | 2 | 21.38 | 19.84 | 49 S1 + S2 | 96 | 4 | 6.11-6.53 | 6.32 |
| 19 | A57331-6 | 2 | 26.19 | 22.4 | 50 S1 + S2 | 96 | 6 | 5.78-6.74 | 6.26 |
| 20 | A57331-8 | 2 | 18.95 | 16.55 | n.c. | n.c. | n.c. | n.c. | n.c. |
| 21 | A57331-9 | 2 | 15.47 | n.c. | n.c. | n.c. | n.c. | n.c. | n.c. |
| 22 | A57331-10 | 2 | 22.13 | 18.49 | 24 S1 + S2 for 1/2 calice | 96 | n.c. | n.c. | n.c. |
| 23 | A57331-11 | 2 | 22.56 | 18.1 | 48 S1 + S2 | 96 | 4 | 5.2-5.8 | 5.5 |
| 24 | A57331-12 | 2 | 15.16 | 11.4 | n.c. | n.c. | n.c. | n.c. | n.c. |
| 25 | 2110A2 | 1 | 21.6 | 18.41 | 48 S1 + S2 | 96 | 4 | 5.22-6.65 | 5.94 |
| 26 | DA2905E2 | 3 | 22.59 | 17.87 | 92 | 92 | 4 | 3.90-4.55 | 4.23 |
| 27 | AM16183 | 1 | 18.34 | 16.11 | 48 for 1/2 calice | 96 | 5 | 5.38-6.15 | 5.77 |
| 28 | PIC-P5310116 | 3 | 17.58 | 15.88 | 104 | 104 | 5 | 3.08-3.41 | 3.25 |
| 29 | PIC-P5290182 | 3 | 12.38 | 11.71 | 19 S1 + S2 for 1/2 calice | 76 | 6.5 | 3.13-3.43 | 3.28 |
| 30 | PIC-P5290125 | 3 | 20.5 | 20 | 48 for 1/2 calice | 96 | 4 | 4.66-5.22 | 9.94 |
| 31 | PIC-P5290123 | 3 | 23.91 | 21.87 | 44 for 1/2 calice | 94 | 4 | 5.26-6.15 | 5.71 |
| 32 | IMG_2112 | 3 | 31.2 | 24 | 90 | 90 | 4 | 6.84-7.66 | 7.25 |
| 33 | PIC-DSC 04139 | 4 | 15.79 | 15.58 | 45 S1 + S2 | 90 | 6 | n.c. | n.c. |
| 34 | PIC-DSC 04656 | 1 | 22.35 | 20 | 52 | 104 | 6 | n.c. | n.c. |
| 35 | PIC-DSC 04331 | 6 | 22 | 19.4 | >40 S1 + S2 | n.c. | 4 | n.c. | n.c. |
| 36 | PIC-DSC 04741 | 1 | 20.91 | 19.55 | >57 | 96 | 4 | 4.78-6.05 | 5.42 |
| 37 | PIC-DSC 04736 | 1 | 21.25 | 20.82 | >52 | 104 | 4 | n.c. | n.c. |
| 38 | PIC-BL 03229 | 6 | 22 | 18.33 | 29 for 1/2 calice | n.c. | n.c. | 6.04-7.16 | 6.6 |

**TABLE 2** (continued).

| 1 | Sample name | Outcrop number | Gd | Sd | Ns | exns | hsd | lS1 | mlS1 |
|---|---|---|---|---|---|---|---|---|---|
| 39 | PIC-BL 03264 | 1 | 13.045 | 12.15 | 40 for 1/2 calice | n.c. | n.c. | 3.51-3.58 | 3.55 |
| 40 | PIC-RV 221965 | 1 | 12.78 | 11.27 | 23 S1 + S2 for 1/2 calice | n.c. | 6 | n.c. | n.c. |
| 41 | PIC-P3170911 | 1 | 23.61 | 17.08 | n.c. | n.c. | 5 | n.c. | n.c. |
| 42 | PIC-DSC 04732 | 1 | 25 | 22.62 | >84 | 93 | 4 | 4.77-5.07 | 4.92 |
| 43 | PIC-P3191196 | 4 | 10.22 | 9.02 | 27 for 1/2 calice | 92 | 6 | 2.21-2.52 | 2.37 |
| 44 | PIC-P3201269 | 1 | n.c. | n.c. | >52 S1 + S | 92 | 4 | 4.27-4.95 | 4.61 |
| 45 | PIC-P3201273 | 1 | n.c. | n.c. | 36 S1 + S2 for 1/2 calice | 120 | n.c. | 4.19-4.66 | 4.43 |
| 46 | PIC-P3191046 | 4 | n.c. | n.c. | >65 | 96 | 5 | n.c. | n.c. |
| 47 | 2303A7-1 | 1 | 27.07 | 19.67 | 44 for 1/2 calice | 88 | 4 | n.c. | n.c. |
| 48 | PIC-P3230535 | 1 | 17.88 | 17.4 | >52 | 105 | 5.5 | 3.07-4.63 | 3.85 |
| 49 | MA0504E3 | 8 | 14.24 | 13.52 | 20 for 1/2 calice | n.c. | 5 | n.c. | n.c. |
| 50 | PIC-CD 50 | 1 | 20.52 | 15.6 | 25 for 1/2 calice | n.c. | n.c. | n.c. | n.c. |
| 51 | PIC-P4050245 | 7 | 17.37 | 16.35 | 48 S1 + S2 | 96 | 6 | n.c. | n.c. |
| 52 | PIC-P4050261 | 7 | 23.09 | 21.38 | 46 S1 + S2 | 92 | 4 | 5.25-6.16 | 5.71 |
| 53 | PIC-P4050251 | 7 | 11.8 | 11.8 | 24 S1 + S2 for 1/2 calice | 96 | 8 | n.c. | n.c. |
| 54 | PIC-P4050137 | 8 | 19.7 | 16.73 | 40 S1 + S2 | 80 | 4 | 5.93-6.27 | 6.1 |
| 55 | PIC-P4050139 | 8 | 13.33 | 13.19 | 20 S1 | 80 | 5.5 | n.c. | n.c. |
| 56 | PIC-P4070376 | 7 | 28.96 | 18.75 | 52 S1 + S2 | 104 | 4 | n.c. | n.c. |
| 57 | PIC-P4050141 | 8 | 17.4 | 14.81 | 46 S1 + S2 | 92 | 6 | 3.37-4.31 | 3.84 |
| 58 | PIC-P4050173 | 8 | 14.12 | 13.34 | 44 S1 + S2 | 88 | 6 | 3.63-4.06 | 3.85 |
| 59 | PIC-P4050157 | 8 | 16.18 | 15.29 | 38 S1 + S2 | 57 | 4 | 3.9-4.34 | 4.12 |
| 60 | PIC-P4050179 | 8 | 13.39 | 13.35 | 38 S1 + S2 | 57 | 6 | 2.16-2.29 | 2.23 |
| 61 | PIC-P4050171 | 8 | 16.65 | 15.12 | 38 S1 + S2 | 57 | 6 | 2.46-3.14 | 2.8 |
| 62 | MA0904E9 | 7 | 26.17 | 23.76 | 25 S1 + S2 for 1/2 calice | 100 | 4 | 7.54-8.37 | 7.96 |
| 63 | PIC-P4070392 | 7 | 28.88 | 22.85 | 46 S1 + S2 | 92 | 4 | 6.27-6.8 | 6.54 |
| 64 | PIC-P4070394 | 7 | 25.78 | 20.32 | 49 S1 + S2 | 98 | 4 | n.c. | n.c. |
| 65 | PIC-P4050159 | 8 | 11.72 | 10.64 | 12 S1 | n.c. | 6 | n.c. | n.c. |
| 66 | PIC-P4050163 | 8 | 13.13 | 9.84 | 41 | n.c. | n.c. | n.c. | n.c. |
| 67 | PIC-P4050183 | 8 | 12.87 | 12.81 | 10 S1 | n.c. | n.c. | n.c. | n.c. |
| 68 | MA0904E7 | 7 | 25.13 | 21.24 | 24 S1 | 98 | 4 | 3.64-4.15 | 3.9 |
| 69 | SB236A---035 | 6 | 20.73 | 19.66 | 43 S1 + S2 | 86 | 5 | 4.95-7.42 | 6.19 |
| 70 | SB238 | 6 | 13.65 | 12.67 | 51 | 102 | 7 | n.c. | n.c. |
| 71 | PIC-P4050131 | 8 | 14.4 | n.c. | 23 for 1/2 calice (S1 + S2) | 92 | 5 | 4.17-4.63 | 4.4 |
| 72 | PIC-P4050151 | 8 | 16.72 | 14.81 | n.c. | n.c. | n.c. | n.c. | n.c. |
| 73 | PIC-P4050153 | 8 | 9.02 | 7.46 | n.c. | n.c. | 10 | n.c. | n.c. |
| 74 | PIC-P4050155 | 8 | 11.9 | 9.96 | n.c. | n.c. | 6 | n.c. | n.c. |
| 75 | PIC-P4050161 | 8 | 7.56 | 7.45 | n.c. | n.c. | 10 | n.c. | n.c. |

**TABLE 2** (continued).

| 1 | Sample name | Outcrop number | Gd | Sd | Ns | exns | hsd | lS1 | mlS1 |
|---|---|---|---|---|---|---|---|---|---|
| 76 | PIC-P4050165 | 8 | 10.15 | 9.58 | n.c. | n.c. | 10 | n.c. | n.c. |
| 77 | PIC-P4050175 | 8 | 15.38 | 11.19 | 37 S1 + S2 | 74 | 5 | 3.82-5.74 | 4.78 |
| 78 | PIC-P4050177 | 8 | 11.4 | n.c. | 16 for 1/2 calice | n.c. | 5 | n.c. | n.c. |
| 79 | PIC-P4050185 | 8 | 17.61 | 14.14 | n.c. | n.c. | 5 | n.c. | n.c. |
| 80 | PIC-P4050187 | 8 | 11.54 | 11.02 | n.c. | n.c. | 7 | n.c. | n.c. |
| 81 | PIC-P4050193 | 8 | 12.61 | 11.54 | n.c. | n.c. | 6 | n.c. | n.c. |
| 82 | PIC-P4050195 | 8 | 9.49 | 8.37 | 37 S1 + S2 | 74 | 8 | 2.50-2.87 | 2.69 |
| 83 | PIC-P4050197 | 8 | 15.65 | 14.69 | 40 S1 + S2 | 80 | 5 | 5.34-5.61 | 5.48 |
| 84 | PIC-P4070330 | 7 | 24.39 | 22.03 | n.c. | n.c. | 4 | n.c. | n.c. |
| 85 | PIC-P4070355 | 7 | 27.4 | n.c. | n.c. | n.c. | 4 | n.c. | n.c. |
| 86 | PIC-P4070378 | 7 | 11.18 | n.c. | n.c. | n.c. | 5 | n.c. | n.c. |
| 87 | PIC-P4070386 | 7 | n.c. | n.c. | n.c. | n.c. | 5 | n.c. | n.c. |
| 88 | MA0904E9 | 7 | 11.77 | 10.98 | n.c. | n.c. | 7 | n.c. | n.c. |
| 89 | PIC-P3230852 | 1 | n.c. | n.c. | n.c. | n.c. | n.c. | n.c. | n.c. |
| 90 | PIC-P3230544 | 1 | n.c. | n.c. | n.c. | n.c. | n.c. | n.c. | n.c. |
| 91 | PIC-P3201301 | 1 | n.c. | n.c. | n.c. | n.c. | n.c. | n.c. | n.c. |
| 92 | SB166 | 6 | 14.48 | 13.01 | 42 | n.c. | 5 | n.c. | n.c. |

tial connections between them. These analyses were conducted with the statistic software PAST (PAleontological STatistics; Hammer et al., 2001). In addition to the classical univariate and bivariate analysis, principal component, correspondence, and discriminant analyses have been performed on three distinct sets of data to maximize the number of samples considered in each analysis (the missing values written “n.c.” in Table 2 rule out the corresponding samples in the analysis). Set 1 includes all the characters (Gd, Sd, exns, hsd, mlS1, mlS2, mlS3, ps, dp) but with a number of only 23 samples. Set 2 includes set 1 but excludes the characters mlS1, mlS2, and mlS3 for a total of 44 samples. Set 3 includes set 1 but excludes the character mls3 for a total of 34 samples in the analysis

In the analysis, the points corresponding to the samples have been differentiated in accordance with the apparent morphology of pseudocolumella observed (point for type 1 and cross for type 2); and sometimes also in accordance with the sampling location.

Three-dimensional CT-scan reconstructions have been created using the nanotom S phoenix 180 kV of Georessources laboratory in Nancy. The X-ray CT is a non-destructive technique used to inspect the internal structure of solid specimen based on recording abnormal attenuations levels of X-rays after passing them through a specimen. The X-ray measurements are dependent on density contrasts within studied specimen (Pryvalov et al., 2017). Two samples (A57331-1 and AM16161) have been chosen for their sufficient density contrasts between skeleton and matrix. Their internal skeletal structure has been observed in the three directions of a defined space as three sets of successive slices perpendicular to each axis of the define space (Figure 2). Successive transverse sections along the height of the corallites of each sample are presented in Appendices 2 and 3.

## SYSTEMATIC PALEONTOLOGY

Phylum CNIDARIA Verrill, 1865
Class ANTHOZOA Ehrenberg, 1834
Sub-Class HEXACORALLIA Haeckel, 1866
Order SCLERACTINIA Bourne, 1900
Sub-Order CARYOPHYLLIINA Vaughan and Wells, 1943
Super-Family VOLZEIOIDEA Melnikova, 1974
Family incertae sedis
*Neorylstonia,* nomen novum pro *Mesophyllum* Beauvais, 1986 non Schlüter, 1889

**TABLE 2** (continued).

| 1 | Sample name | Outcrop number | IS2 | mIS2 | IS3 | mIS3 | ps | pd | nps |
|---|---|---|---|---|---|---|---|---|---|
| 2 | AM16177 | 1 | n.c. | n.c. | n.c. | n.c. | n.c. | 7.6 | n.c. |
| 3 | A57331-1 | 2 | 3.39-4.51 | 3.95 | 1.32-2.26 | 1.79 | 1 | 7.3 | 26 |
| 4 | AM16160 | 1 | 4.03-4.45 | 4.24 | 1.89-2.04 | 1.92 | 2 | 6.33 | 21 |
| 5 | AM16164 | 1 | 3.95-4.45 | 4.2 | n.c. | n.c. | 2 | 7.76 | n.c. |
| 6 | AM16164 bis | 1 | 3.01-3.32 | 3.17 | n.c. | n.c. | 2 | 5.7 | n.c. |
| 7 | DA2905E1.1 | 3 | 6.16-6.51 | 6.34 | 3.1-3.9 | 3.5 | 1 | 9.7 | n.c. |
| 8 | 2703A6 | 1 | n.c. | n.c. | n.c. | n.c. | 1 | 12.56 | 25 |
| 9 | AM16172 | 4 | 5.15-5.56 | 5.36 | 2.42-2.85 | 2.64 | n.c. | 9.44 | n.c. |
| 10 | AM16161 | 1 | 3.48-3.53 | 3.51 | 1.51-1.70 | 1.61 | 2 | 6.5 | n.c. |
| 11 | A30500-1 | 5 | n.c. | n.c. | n.c. | n.c. | n.c. | n.c. | n.c. |
| 12 | A30500-2 | 5 | n.c. | n.c. | n.c. | n.c. | n.c. | n.c. | n.c. |
| 13 | A30500-3 | 5 | n.c. | n.c. | n.c. | n.c. | n.c. | n.c. | n.c. |
| 14 | A30500-4 | 5 | n.c. | n.c. | n.c. | n.c. | n.c. | n.c. | n.c. |
| 15 | AM16175 | 4 | 3.30-4.00 | 3.65 | 0.67-1.21 | 0.74 | 1 | 6.56 | 15 |
| 16 | A57331-2 | 2 | n.c. | n.c. | n.c. | n.c. | 1 | 7.75 | >21 |
| 17 | A57331-4 | 2 | n.c. | n.c. | n.c. | n.c. | 1 | 7 | n.c. |
| 18 | A57331-5 | 2 | 5.51-5.80 | 5.66 | 1.98-2.26 | 2.12 | 1 | 7.72 | 18 |
| 19 | A57331-6 | 2 | 5.14-5.86 | 5.5 | n.c. | n.c. | n.c. | n.c. | n.c. |
| 20 | A57331-8 | 2 | n.c. | n.c. | n.c. | n.c. | 1 | 6.39 | 21 |
| 21 | A57331-9 | 2 | n.c. | n.c. | n.c. | n.c. | 2 | 5.21 | n.c. |
| 22 | A57331-10 | 2 | n.c. | n.c. | n.c. | n.c. | 1 | 8.24 | 23 |
| 23 | A57331-11 | 2 | 4.7-5.0 | 4.85 | 2.4-2.7 | 2.55 | 1 | 9.86 | 23 |
| 24 | A57331-12 | 2 | n.c. | n.c. | n.c. | n.c. | 1 | n.c. | n.c. |
| 25 | 2110A2 | 1 | 4.76-5.53 | 5.15 | 2.19-2.70 | 2.45 | 2 | 7.83 | n.c. |
| 26 | DA2905E2 | 3 | 3.08-3.99 | 3.54 | 1.77-2.14 | 1.96 | 1 | 6.41 | >17 |
| 27 | AM16183 | 1 | 4.51-5.46 | 4.99 | 1.98-2.71 | 2.35 | 2 | 6.99 | n.c. |
| 28 | PIC-P5310116 | 3 | 2-2.91 | 2.46 | 0.62-1.24 | 0.93 | 2 | 6.24 | n.c. |
| 29 | PIC-P5290182 | 3 | 2.94-3.13 | 3.04 | 1.87-2.34 | 2.11 | 2 | 4.5 | n.c. |
| 30 | PIC-P5290125 | 3 | 4.36-4.75 | 4.56 | 2.02-2.54 | 2.28 | 1 | 7 | 20 |
| 31 | PIC-P5290123 | 3 | 4.99-5.67 | 5.33 | 2.58-3.30 | 2.94 | n.c. | n.c. | n.c. |
| 32 | IMG_2112 | 3 | 6.12-6.65 | 6.39 | 3.31-4.03 | 3.67 | 1 | 12.48 | 25 |
| 33 | PIC-DSC 04139 | 4 | n.c. | n.c. | n.c. | n.c. | 2 | 7.16 | n.c. |
| 34 | PIC-DSC 04656 | 1 | n.c. | n.c. | n.c. | n.c. | 1 | 8.24 | 24 |
| 35 | PIC-DSC 04331 | 6 | n.c. | n.c. | n.c. | n.c. | 2 | 6 | n.c. |
| 36 | PIC-DSC 04741 | 1 | 4.45-5.11 | 4.78 | 2.68-3.27 | 2.98 | 1 | 8.18 | 21 |
| 37 | PIC-DSC 04736 | 1 | n.c. | n.c. | n.c. | n.c. | 2 | 10.51 | n.c. |
| 38 | PIC-BL 03229 | 6 | 3.97-5.23 | 4.6 | 2.46-2.74 | 2.6 | 2 | 6.44 | 25 |
| 39 | PIC-BL 03264 | 1 | 2.75-2.78 | 2.77 | 1.50-2.08 | 1.79 | 2 | 5.07 | n.c. |
| 40 | PIC-RV 221965 | 1 | n.c. | n.c. | n.c. | n.c. | 2 | 5.56 | n.c. |
| 41 | PIC-P3170911 | 1 | n.c. | n.c. | n.c. | n.c. | 2 | 9.03 | >18 |

**TABLE 2** (continued).

| 1 | Sample name | Outcrop number | IS2 | mIS2 | IS3 | mIS3 | ps | pd | nps |
|---|---|---|---|---|---|---|---|---|---|
| 42 | PIC-DSC 04732 | 1 | 4.3-4.5 | 4.4 | 2.4-3.8 | 2.9 | 1 | 9.52 | 24 |
| 43 | PIC-P3191196 | 4 | 1.6-2.01 | 1.81 | 0.93-0.97 | 0.95 | 1 | 4.09 | 19 |
| 44 | PIC-P3201269 | 1 | 3.92-4.45 | 4.19 | 2.26-2.85 | 2.56 | 1 | n.c. | >16 |
| 45 | PIC-P3201273 | 1 | 3.69-4.36 | 4.03 | 1.43-1.73 | 1.58 | 2 | n.c. | n.c. |
| 46 | PIC-P3191046 | 4 | n.c. | n.c. | n.c. | n.c. | 1 | n.c. | 25 |
| 47 | 2303A7-1 | 1 | n.c. | n.c. | n.c. | n.c. | 1 | 5.9 | 20 |
| 48 | PIC-P3230535 | 1 | 3.04-3.56 | 3.3 | 1.35-1.83 | 1.59 | 1 | 6.45 | 21 |
| 49 | MA0504E3 | 8 | n.c. | n.c. | n.c. | n.c. | 2 | 5 | n.c. |
| 50 | PIC-CD 50 | 1 | n.c. | n.c. | n.c. | n.c. | 1 | n.c. | >21 |
| 51 | PIC-P4050245 | 7 | n.c. | n.c. | n.c. | n.c. | 1 | 5.09 | n.c. |
| 52 | PIC-P4050261 | 7 | 4.68-5.24 | 5.96 | 3.22-3.66 | 3.44 | 1 | 9.31 | >20 |
| 53 | PIC-P4050251 | 7 | n.c. | n.c. | n.c. | n.c. | n.c. | 4.54 | n.c. |
| 54 | PIC-P4050137 | 8 | 4.91-5.10 | 5.01 | n.c. | n.c. | 2 | 5.98 | n.c. |
| 55 | PIC-P4050139 | 8 | n.c. | n.c. | n.c. | n.c. | 2 | 4.3 | n.c. |
| 56 | PIC-P4070376 | 7 | n.c. | n.c. | n.c. | n.c. | 1 | 9.71 | 22 |
| 57 | PIC-P4050141 | 8 | 1.84-2.78 | 2.36 | n.c. | n.c. | 2 | 4.34 | n.c. |
| 58 | PIC-P4050173 | 8 | 2.05-2.96 | 2.51 | n.c. | n.c. | 2 | 5.07 | n.c. |
| 59 | PIC-P4050157 | 8 | 2.63-3.37 | 3 | n.c. | n.c. | 2 | 6.41 | n.c. |
| 60 | PIC-P4050179 | 8 | 0.99-1.23 | 1.11 | n.c. | n.c. | 2 | 4.54 | n.c. |
| 61 | PIC-P4050171 | 8 | 1.45-1.78 | 1.62 | n.c. | n.c. | 2 | 4.7 | n.c. |
| 62 | MA0904E9 | 7 | 6.28-7.25 | 6.77 | 4.55-4.67 | 4.61 | 1 | 7.76 | 23 |
| 63 | PIC-P4070392 | 7 | 5.78-6.03 | 5.91 | 2.34-3.18 | 2.76 | 1 | 11.88 | 20 |
| 64 | PIC-P4070394 | 7 | n.c. | n.c. | n.c. | n.c. | n.c. | 7.64 | n.c. |
| 65 | PIC-P4050159 | 8 | n.c. | n.c. | n.c. | n.c. | 2 | 3.97 | n.c. |
| 66 | PIC-P4050163 | 8 | n.c. | n.c. | n.c. | n.c. | 2 | 3.04 | n.c. |
| 67 | PIC-P4050183 | 8 | n.c. | n.c. | n.c. | n.c. | 2 | 4.03 | n.c. |
| 68 | MA0904E7 | 7 | 2.73-3.08 | 2.91 | 1.15-1.60 | 1.38 | 1 | 8.93 | 25 |
| 69 | SB236A---035 | 6 | 3.84-5.80 | 4.82 | 2.31-3.14 | 2.73 | 2 | 5.6 | n.c. |
| 70 | SB238 | 6 | n.c. | n.c. | n.c. | n.c. | 1 | 5.04 | >13 |
| 71 | PIC-P4050131 | 8 | 2.67-3.49 | 3.08 | n.c. | n.c. | 2 | 5.08 | n.c. |
| 72 | PIC-P4050151 | 8 | n.c. | n.c. | n.c. | n.c. | 2 | 7.02 | n.c. |
| 73 | PIC-P4050153 | 8 | n.c. | n.c. | n.c. | n.c. | 2 | 2.69 | n.c. |
| 74 | PIC-P4050155 | 8 | n.c. | n.c. | n.c. | n.c. | 2 | 3.52 | n.c. |
| 75 | PIC-P4050161 | 8 | n.c. | n.c. | n.c. | n.c. | 2 | 2.01 | n.c. |
| 76 | PIC-P4050165 | 8 | n.c. | n.c. | n.c. | n.c. | 2 | n.c. | >19 |
| 77 | PIC-P4050175 | 8 | 2.94-4.56 | 3.75 | n.c. | n.c. | 2 | 6.76 | n.c. |
| 78 | PIC-P4050177 | 8 | n.c. | n.c. | n.c. | n.c. | 2 | 5.78 | n.c. |
| 79 | PIC-P4050185 | 8 | n.c. | n.c. | n.c. | n.c. | 2 | 5.78 | n.c. |
| 80 | PIC-P4050187 | 8 | n.c. | n.c. | n.c. | n.c. | 2 | 3.34 | n.c. |
| 81 | PIC-P4050193 | 8 | n.c. | n.c. | n.c. | n.c. | 2 | 3.42 | n.c. |

**TABLE 2** (continued).

| 1 | Sample name | Outcrop number | lS2 | mlS2 | lS3 | mlS3 | ps | pd | nps |
|---|---|---|---|---|---|---|---|---|---|
| 82 | PIC-P4050195 | 8 | 1.66-1.83 | 1.75 | n.c. | n.c. | 2 | 3.09 | n.c. |
| 83 | PIC-P4050197 | 8 | 3.26-3.7 | 3.48 | n.c. | n.c. | 2 | 4.76 | n.c. |
| 84 | PIC-P4070330 | 7 | n.c. | n.c. | n.c. | n.c. | 1 | 5.42 | n.c. |
| 85 | PIC-P4070355 | 7 | n.c. | n.c. | n.c. | n.c. | n.c. | 9.63 | n.c. |
| 86 | PIC-P4070378 | 7 | n.c. | n.c. | n.c. | n.c. | 1 | 3.85 | n.c. |
| 87 | PIC-P4070386 | 7 | n.c. | n.c. | n.c. | n.c. | n.c. | n.c. | n.c. |
| 88 | MA0904E9 | 7 | n.c. | n.c. | n.c. | n.c. | 1 | 3.74 | n.c. |
| 89 | PIC-P3230852 | 1 | n.c. | n.c. | n.c. | n.c. | 2 | n.c. | n.c. |
| 90 | PIC-P3230544 | 1 | n.c. | n.c. | n.c. | n.c. | 2 | n.c. | n.c. |
| 91 | PIC-P3201301 | 1 | n.c. | n.c. | n.c. | n.c. | 2 | n.c. | n.c. |
| 92 | SB166 | 6 | n.c. | n.c. | n.c. | n.c. | 2 | 4.4 | n.c. |

**Type species.** *Mesophyllum pseudocolumellatum* Beauvais, 1986.

**Derivatio nominis.** *Neorylstonia* in reference to its doppelganger Paleozoic *Rylstonia*

**Nomenclatural remarks.** *Mesophyllum* Beauvais, 1986, is a junior homonym of *Mesophyllum* Schlüter, 1889 (p. 67). Unfortunately, as already indicated, several other junior homonyms were reported and among them another Liassic coral. The genus *Mesophyllum* Hahn, 1911 (p. 555), is a junior homonym of *Mesophyllum* Schlüter, 1889 (p. 67). *Archaeosmilia* Melnikova, 1975, could be an available synonym but a comparison with the type material is still necessary. If these two genera are justified in terms of taxonomy, a *nomen novum* should be created for *Mesophyllum* Hahn. Another junior homonym is also reported with the mention of "*Mesophyllum* Barrois, 1889 (see Barrois, 1889, p. 67)" by Neave (1940, p. 119). This quotation was present in other earlier indexes (e.g., Waterhouse, 1902, p. 219), but the citation could not be found in the 1888 nor the 1889 works of Barrois. Nevertheless, Barrois (1898, p. 241) gave a faunal list with "*Mesophyllum lissingenense*, Schlu." [Schlüter] and "*Mesophyllum* nov. sp."; the latter of which might be the origin of the erroneous entry. In conclusion, for these reasons, "*Mesophyllum* Barrois" is unavailable. *Mesophyllum* Hahn, 1911, is also a senior homonym of *Mesophyllum* Vieira, 1942, and *Mesophyllum* Beauvais, 1986, all of them depending on the zoological code. Incidentally, *Mesophyllum* is also the name of a red alga.

The family is given as incertae sedis because this taxon presents some characters of both Gardineriidae and Volzeiidae. The genus shares smooth lateral faces of septa with the Gardineriidae but differs to them by the presence of an endotheca; and the microstructure of septa is close to the one of Volzeiidae (according to the description of *Volzeia badiotica* in Cuif, 1974) but with no lateral spines or granulation.

*Neorylstonia pseudocolumellata* (Beauvais, 1986)

v. 1986 *Mesophyllum pseudocolumellatum* Beauvais, 1986, p. 20, Pl. 4, fig. 1a-1b

**zoobank.org/52069B98-79EA-4F0E-AD01-C1EFF035D5F2**

**Originally included material.** 7 specimens.

**Type designation.** *Mesophyllum pseudocolumellatum* Beauvais, 1986 MNHN.F.R11604, Menchikoff collection. Holotype by original designation Beauvais, 1985, p. 20, figured plate 4 figure 1a, 1b; Paratypes figured plate 4, figure 1c, d and e.

**Type locality.** Beni Tadjit, Lower Jurassic.

**Status.** Available and valid.

**Dimensions.** Great diameter: 9–29 mm, Small diameter: 7.5–22.1 mm, Number of septa: 41–104 (mostly around 96), Septal density (S1 + S2): 4–10 for 5 mm.

**Description.** Solitary coral. Corallum ceratoid, straight, or curved. The calice is subcircular in outline. Costosepta straight or slightly curved (possibly post-mortem distortion), free, compact, occasionally rhopaloid. Some first-order (S1) septa rarely reach the axial structure but in most cases the inner edge abruptly dips in the fossa (see Figure 3.1-2). Lateral faces and distal edge are smooth. No palus. Radial elements are commonly arranged in three distinct size orders with different length and width in transverse sections but S1 and S2 are occasionally indistinct because of similar

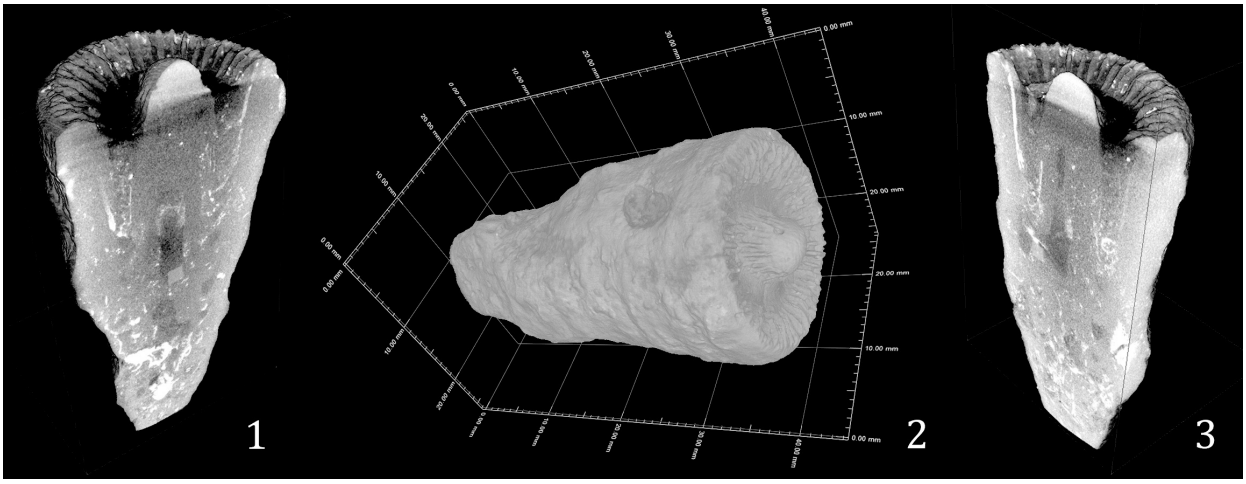


**FIGURE 2.** Examples of CT scan images provided by nanotom S phoenix 180 kV analysis on sample A57331-1. The slices through the coral presented in **1** and **3** are perpendicular to each other and parallel to their corresponding plan materialized by white dotted lines in **2**. The annotated graduations in **2** are centimeters.

sizes. In contrast, some other samples show four clearly distinguishable size orders of septa. In the latter case, the first and second size orders geometrically correspond to a subdivision of the S1. Lastly, the S3 are sometimes missing.

On the basis of the described arrangement of septal length and thicknesses a very classical model of septal insertion can be proposed, namely 96 septa distributed in five ontogenetical cycles according to 6+6+12+24+48 septa (see Figure 4). This model of septal insertion is statistically significant by univariate statistical analysis, in which the number 96 shows a well-marked mode. Ghosts of septal structures can sometimes be observed in thin sections (Figure 3.4). They consist in transverse section of a darker axial zone within the septum, a brighter zigzag line or some dark spots in a line considered as remains of “centers of calcification” or centers of rapid accretion (Stolarski, 2003). Growth lines in “ogive” or “gloves fingers” can be seen in longitudinal sections, resulting from the deposition of different successive layers of stereome thickening the septa (thickening deposits of Stolarski, 2003).

Axial structure is present, in the form of a Rugose-like calicular boss made of septa and endotheca. This pseudocolumella presents different morphologies throughout the polyp’s life (Figure 5, Appendices 1-3), giving the fossils a very characteristic aspect in transverse section. The pseudocolumella is made of 16 to 26 septal lamellae that seem to correspond to septa in some samples but, contrary to the septal system, are organized in a bilateral symmetry rather than the strict radial symmetry. Tabulae in the axial porosity (when present) and dissepiments between the lamellae sustain this structure. Most commonly the pseudocolumella consists, on average, of 21 to 22 lamellae organized in two main skeletal morphologies: Type 1 morphology—lamellae organized in the form of a star with opposite septa sometimes linked in the calicular axial zone (Figure 5.3). In some cases, the bilateral symmetry plan is materialized by a stereome deposit between lamellae, which should not be confused with a rugose-like axial lamellae (Figure 6.6). Type 2 morphology—lamellae organized in two soft crescents (the cross sections look like two kidney beans, see Figure 5.12) separated by an axial cavity regularly sealed by tabulae, which seem to serve as basis for the genesis of new lamellae (Figure 6.2). These tabulae probably correspond to stasis phases in the growth of the polyp alternating with stages of vertical increase associated with the secretion of lamellae by the soft ectodermal tissues of the animal.

Between these two extreme morphologies are some transitional states (Figure 5), and both morphologies sometimes coexist in one single sample. In such cases, the pseudocolumella always shows the same ontogenic pattern starting with a type 2 morphology in the early stages of development then vertically turning to a type 1 morphology in the oldest stages of development. Once the type 1 morphology is established, it never transforms (back) to type 2. Another point is that type 1 pseudocolumella are associated with a more conical shape of the corallite and, in this conformation, the axial structure continues to grow when the vertical increase of the wall stopped, sometimes highly surpassing the calix rim (Figure 6.9-11).

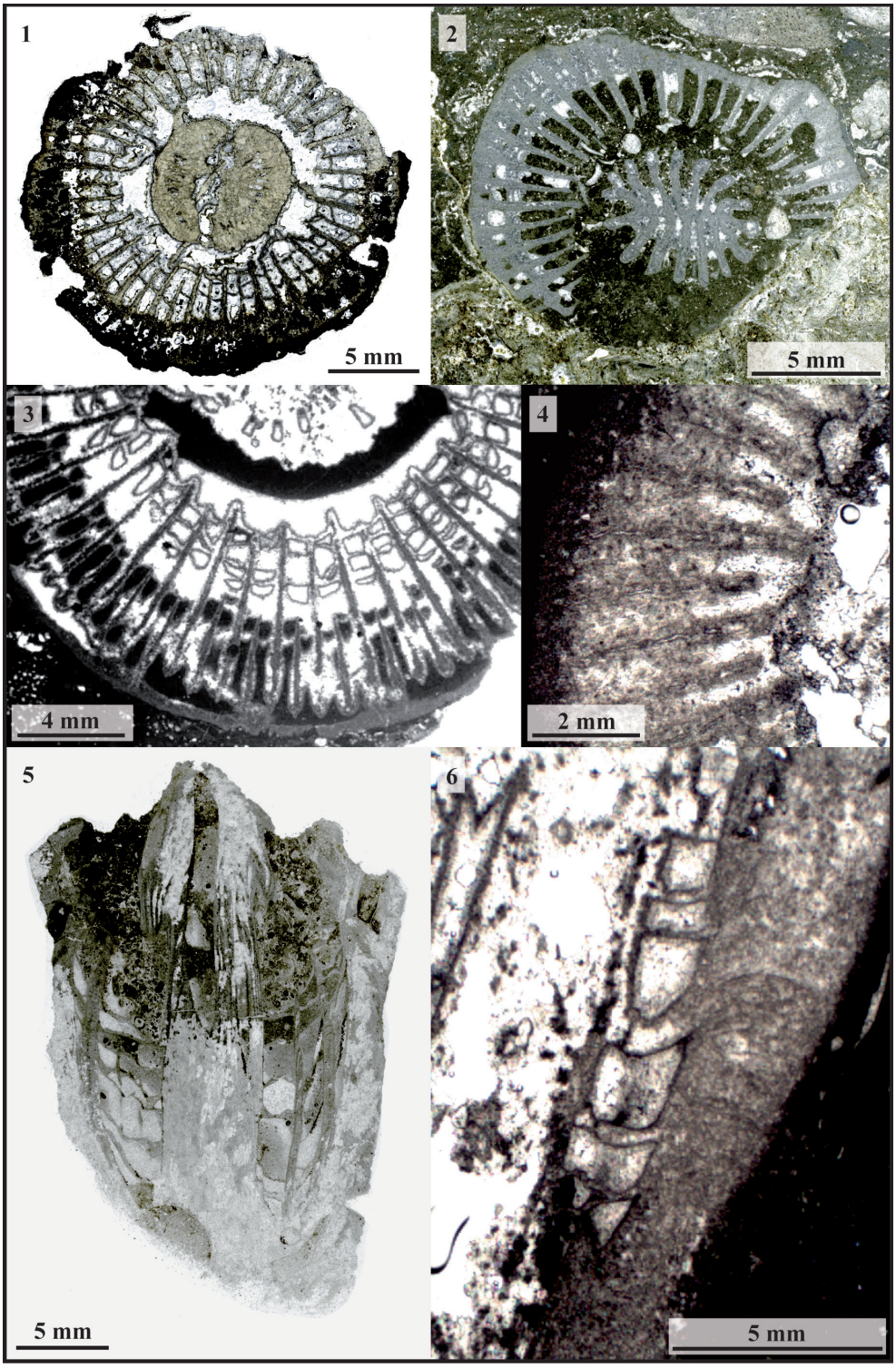


**FIGURE 3.** Photographs of *Neorylstonia pseudocolumellata*. **1,** Transverse section of the sample AM16164-2 showing a type 2 pseudocolumella with visible pseudocolumellar septa. **2,** Transverse section of sample AM175 showing a type 1 pseudocolumella. **3,** Transverse section in sample DA2905E1.1 showing the true epitheca surrounding the septal apparatus and the stereome deposits on septa. **4,** Detail of the ghosts of septal structure in transverse section (sample 2110A2) and the stereome deposits in "ogives" or "glove fingers". **5,** Longitudinal section of sample A57331-2 showing the endothecal organization in tabular dissepiments and the axial porosity of the pseudocolumella. **6,** Detail of the parathecal wall in continuity with the tabular dissepiments (longitudinal section of sample 2110A2).

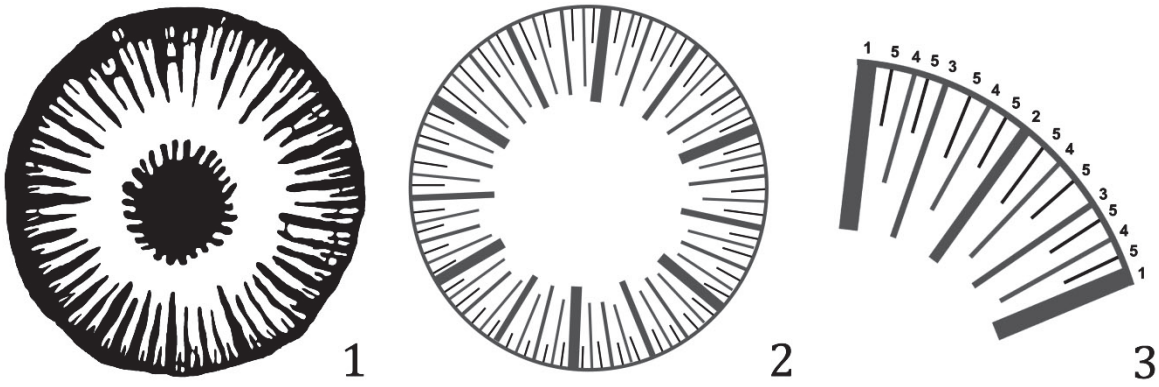


**FIGURE 4.** Model of septal insertion based on the sample A57331-1. **1,** Septal organization of the sample A57331-1. **2,** Geometrical interpretation of the septal apparatus of the sample. **3,** Detail of one of the six systems of the corallite including the five supposed ontogenetic cycles. In most samples these ontogenetic cycles are inferred from morphology by the three distinct size orders: size order 1 includes cycles **1, 2 and 3**; order 2 includes cycle 4 and order 3 includes cycle 5. In very few samples only, ontogenetic cycles **1, 2 and 3** can be differentiated.

Type 2 pseudocolumella never surpass the distal edges of septa and are associated with more cylindrical corallite shapes suggesting a continuous growth during the animal's life.

The pseudocolumella is generally wrapped into continuous deposits of stereome, which separate it from the lumen. It is observed independently of the morphology of the axial structure (Figure 6.3-5) and excludes the possibility of post-secretion modifications of the skeleton to explain the variations observed in morphologies (for example a case of symbiosis associated with specific bioero-

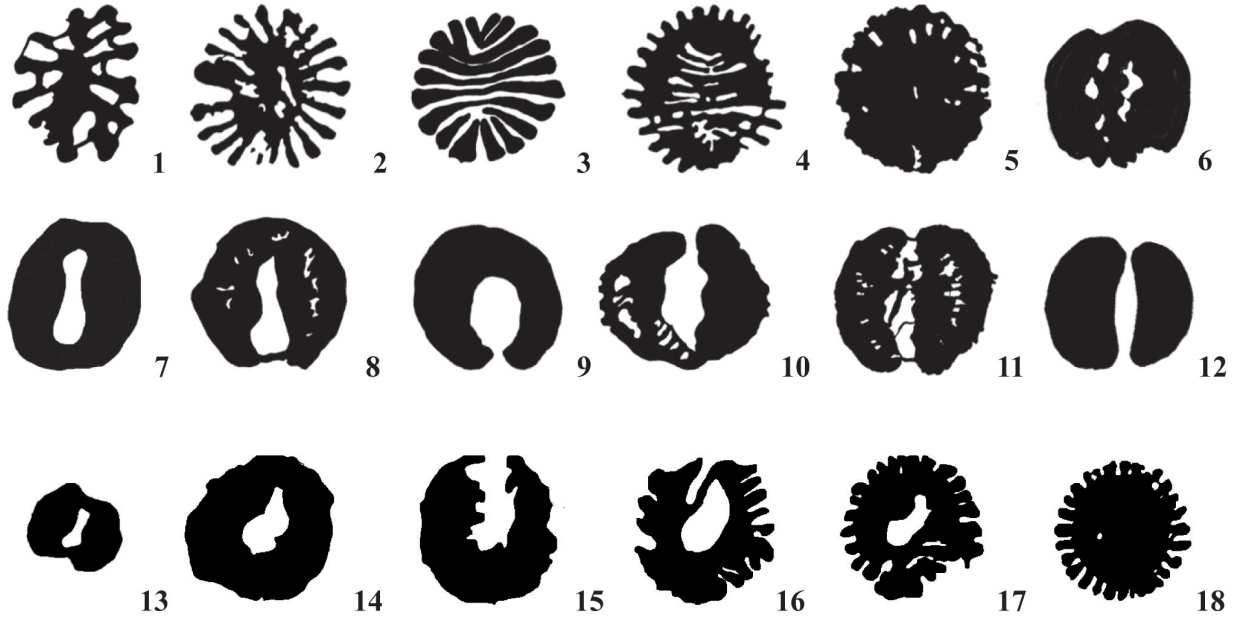


**FIGURE 5.** Schematic representations of the different shapes of pseudocolumella observed among the samples (**1-12**) or in one single sample, from the base to the top (**13-18**). Shapes **1, 2, 3, 4, 5, 17 and 18** correspond to type 1 morphology and shapes **6, 7, 8, 9, 10, 11, 12, 13, 14, 15 and 16** correspond to the type 2 morphology.

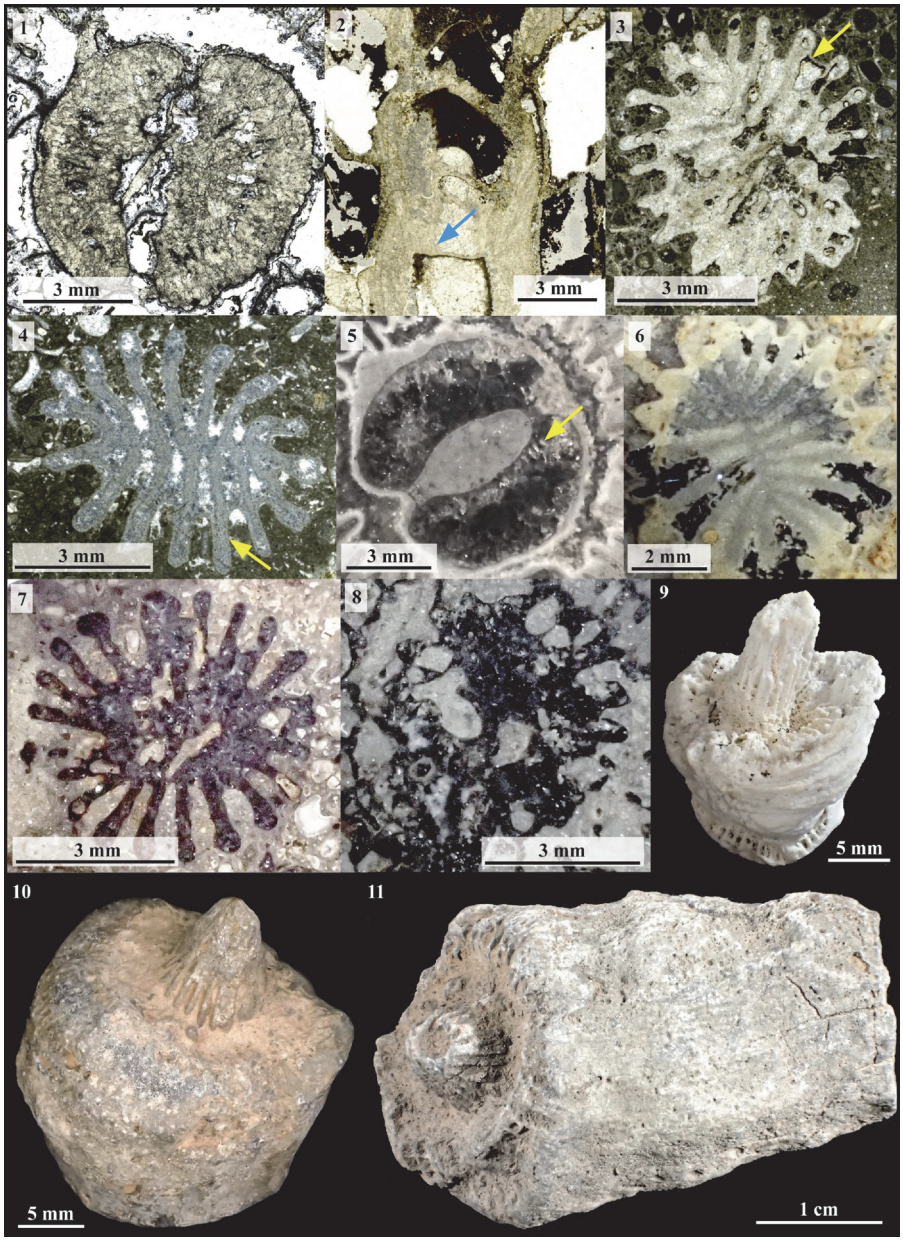


**FIGURE 6.** Plate of photographs of *Neorylstonia pseudocolumellata* focusing on the pseudocolumella structure. **1,** Transverse section of the sample AM16164-1, showing a type 2 pseudocolumella with visible pseudocolumellar septa. **2,** Longitudinal section of the type 2 pseudocolumella AM16164-1. Note the regular tabulae in the axial porosity and the way it sustains new lamellae (arrow). **3,** Transverse section of the sample 2303A7, showing a type 1 pseudocolumella with curved lamellae connected following a bilateral plan of symmetry. An incomplete stereome deposit can be observed around the pseudocolumella (arrow). **4,** Transverse section of the sample AM175, showing a type 1 pseudocolumella with curved lamellae connected following a bilateral plan of symmetry. A complete stereome deposit separate the pseudocolumella lamellae from the lumen (arrow). **5,** Transverse polished section of the sample AM16160 with a type 2 pseudocolumella with crescents connected by endothecal structures. Note the radiant structure into the crescents made of lamellae (arrow) attenuated at their periphery by the stereome deposits. **6,** Transverse polished section of the sample A57331-5 with a type 1 pseudocolumella showing stereome deposits in the bilateral symmetry plan imitating an axial lamellae. **7 and 8,** transverse polished section of the sample 2303A7-1 sectioned at the top (**7**) and at the basis (**8**). The early stages of development at the basis present a rudimentary type 2 pseudocolumella (modified by bioerosion) while the later stage of development shows a type 1 pseudocolumella. **9-11,** Photographs in lateral views of 3 specimens of *N. pseudocolumellata* with a type 1 pseudocolumella surpassing the distal peripheral edges of the calix (respectively, A30500, a paratype from the collections of the Muséum d'Histoire Naturelle de Paris, A57331-8, and A57331-2).

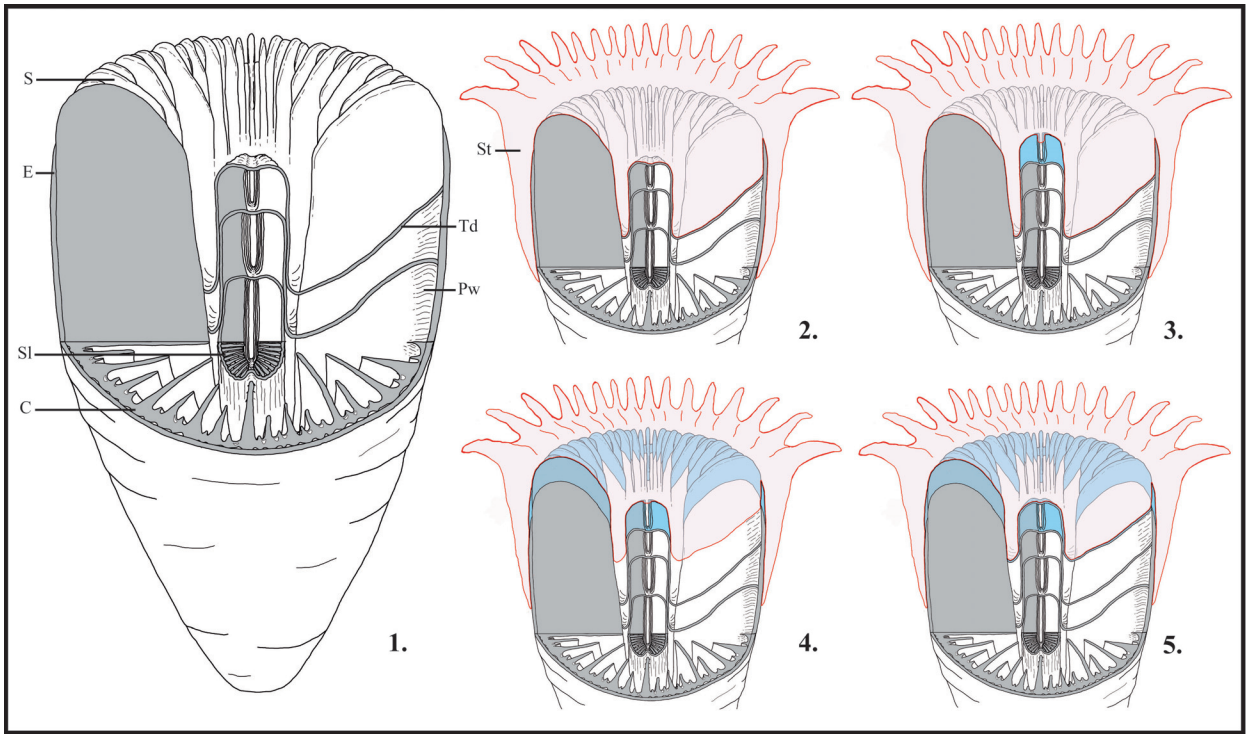


**FIGURE 7.** Step-by-step model of growth for *Neorylstonia pseudocolumellata* based on the assumption of an upward migration of polyp soft tissues by muscular contraction in accordance with structural observations of Brahmi et al. (2012) on dissepiments. Alternative modes of growth for soft tissues exist in the literature but do not impact the skeletal growth in the model (see Chevalier, 1987). **1,** Coral skeleton without soft tissues. **2,** Between two cycles of growth, soft tissues (in red) sit on the tabular dissepiments. **3,** Initiating a new cycle of growth, soft tissues raise above the pseudocolumella and cristallize a new set of septal lamellae (in blue). In this case, relaxed soft tissues above the pseudocolumella produce an axial fold resulting in a type 2 pseudocolumella. **4,** Soft tissues lift up, and simultaneously raise the septal and epithecal edges and raise the parathecal wall at the periphery of the corallite. At this stage, soft tissue is suspected to lift up by (i) septal traction of the growing septa or by (ii) standing on the pseudocolumella and successive stereome deposits forming the parathecal wall or even by (iii) floating on a gas of fluid blister separating the basal rim of the polyp and the tabular dissepiment (see Wells, 1969). **5,** At the end of the growing cycle, new tabular dissepiments are synthetized in contact with the basal epiderm of the polyp. The model is the same for a type 1 pseudocolumella but septal lamellae are connected in the axis. The step-by-step growing phases presented here are a simplified proposition to help the understanding of the reader, the exact details of the coral's growth process 183 million years ago may have been different. Abbreviations: C, costa; E, epitheca; Pw, parathecal wall; S, septa; Sl, septal lamellae; St, soft tissues; Td, tabular dissepiment.

sion is excluded). These stereome deposits attenuate the spiky aspect of the pseudocolumella periphery in cross section. A model of step-by-step skeletal growth is proposed in Figure 7.

In most cases, hexameral symmetry can be established on the basis of the different septa systems. The superimposed bilateral symmetry is evidenced by the spatial organization of the axial structure. Endotheca abundant and made of tabular dissepiments regularly arranged in the axial zone. Parathecal wall is present and the paratheca is continuous with the dissepiments. Synapticulae absent. A true epitheca with growth striae and wrinkles encloses the corallite (Figure 3.3).

As *Neorylstonia* is monospecific, the specific diagnosis is identical to the generic diagnosis.

**Range.** Uppermost Sinemurian (Raricostatum ammonite chronozone) to uppermost Pliensbachian (Spinatum ammonite Chronozone), with a probable acme during Late Pliensbachian (Domerian).

**Occurrence.** High Atlas and Middle Atlas of Morocco

## STATISTICAL APPROACH

### Univariate and Bivariate Analyses

A number of trends can be deduced from the univariate and bivariate analysis (Figure 8). As it

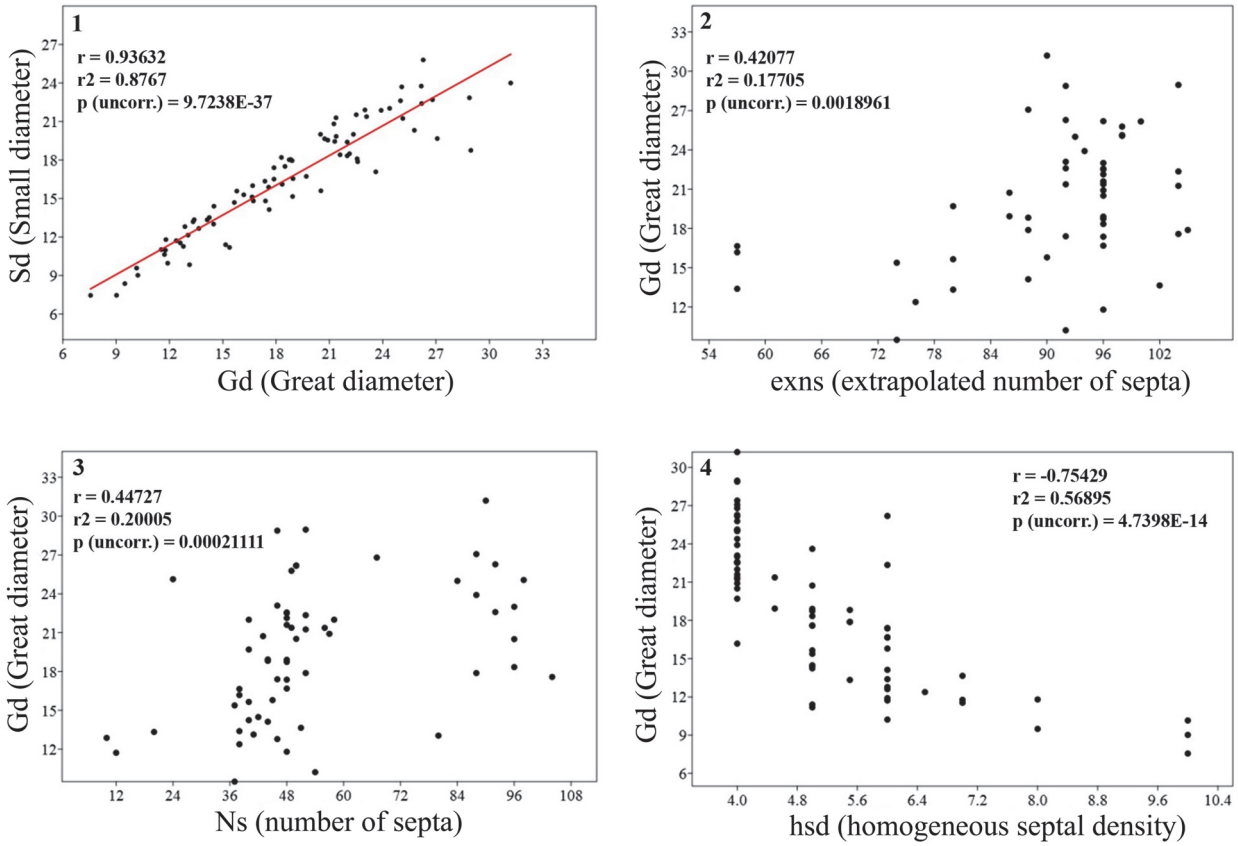


**FIGURE 8.** Univariate analysis based on the data in Table 2. **1,** Small diameter (Sd) as a function of great diameter (Gd). **2,** Great diameter (Gd) as a function of the extrapolated number of septa (exns). **3,** Great diameter (Gd) as a function of the number of septa (Ns). **4,** Great diameter (Gd) as a function of homogeneous septal density.

appears in Figure 8.2, the extrapolated number of septa (exns) seems to increase to some extent with the increase of the calicular diameter, but the link between these two characters is moderate (r = 0.42077), which is quite unexpected for scleractinian corals. A part of this weak correlation between diameters and number of septa is probably related either to a preservation bias or ontogeny. The process of extrapolation of the number of septa can result in an overestimation of the true number of septa in the sample; this may also erase the gradual establishment of the different orders of septa during the growth of the corallum. On the other hand, the apparent number of septa can lead to an underestimate of the true number of septa if some are hidden or broken. Nevertheless, a similar weak correlation is obtained with the non-extrapolated number of apparent septa in the samples (Figure 8.3). The points in Figure 8.3 are grouped in four packages (samples having approximately 12, 24, 48, and 96 septa) corresponding to different stages of development of the septal apparatus in the samples (see Figure 4), but all the samples from the package corresponding to approximately 48 septa in the septal apparatus could potentially be corals with a hidden third order of septa. Consequently, the possibility of making different species from these three packages, as old typological methods could have done, is not advised. Finally, the only conclusion that can be drawn from the values in Figures 8.2 and 8.4 is that *N. pseudocolumellata* develops its three orders even with small calicular diameters. This supports the idea that the growth size of the coral is more influenced by environmental parameters than the number of septa, which could be more linked to age.

The homogeneous septal density (hsd) is very clearly negatively correlated with the calicular diameter (Figure 8.4). As demonstrated in Figure 9.5 the main number of extrapolated septa conforms well to the model with 96 septa exposed in the diagnosis. Figures 9.4, 9.5, and 9.6 emphasize the correlation between the length of septa from one cycle of septa to another cycle of septa.

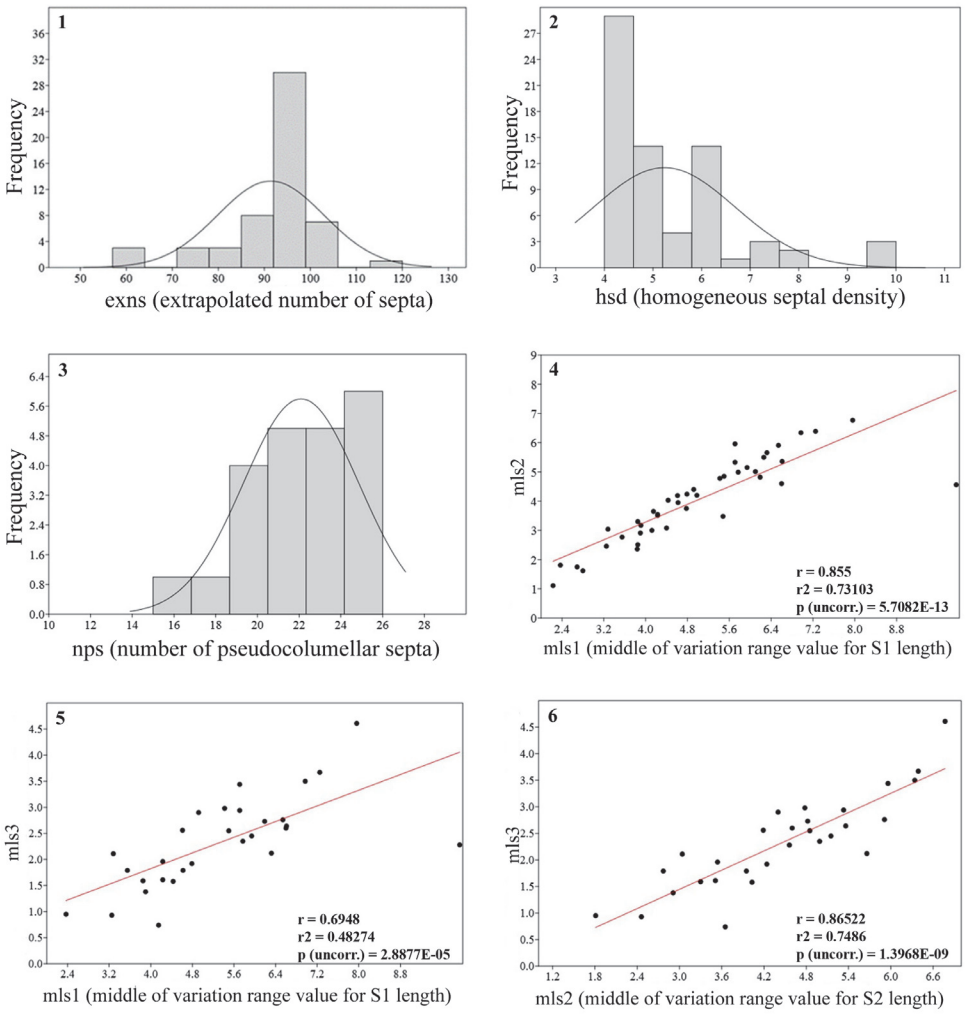


**FIGURE 9.** Univariate analysis based on the data in Table 2. **1,** Frequencies of the values of extrapolated number of septa (exns). **2,** Frequencies of the values of homogeneous septal density (hsd). **3,** Frequencies of the values of number of pseudocolumellar septa (nps). **4,** Middle of variation range value of S1 length as a function of the middle of variation range value of S2 length. **5,** Middle of variation range value of S2 length as a function of the middle of variation range value of S3 length. **6,** Middle of variation range value of S3 length as a function of the middle of variation range value of S1 length. The r value corresponds to the linear correlation coefficient and P (uncorr.) value represents the probability of having no correlation between the two compared sets of data.

## Multivariate Analyses

Principal components analysis (PCA) gave a sum of variance percentages greater than 93% for PC1 + PC2 in every set of data considered. The most influential character is the extrapolated number of septa (exns) in each case, followed by the great calicular diameter (Gd) and small calicular diameter (Sd) and after come the pseudocolumella diameter (dp) and the middle of variation range values for length of septa (mls1–3). The major role of dimensions and number of septa in PCA results is already well known for corals and corresponds to the traditional measurements used in taxonomy since the nineteenth century. Interestingly, the samples with a type 1 pseudocolumella are associated to high diameters and number of septa when the samples with a type 2 pseudocolumella correspond to high homogeneous septal density values and smaller calicular diameters (Figure 10). Similar results are observed with correspondence analysis and discriminant analysis, and the same trends are recorded for each set of data. Discriminant analysis gives one more important piece of information as it shows an “outcrop effect”; the corals from a

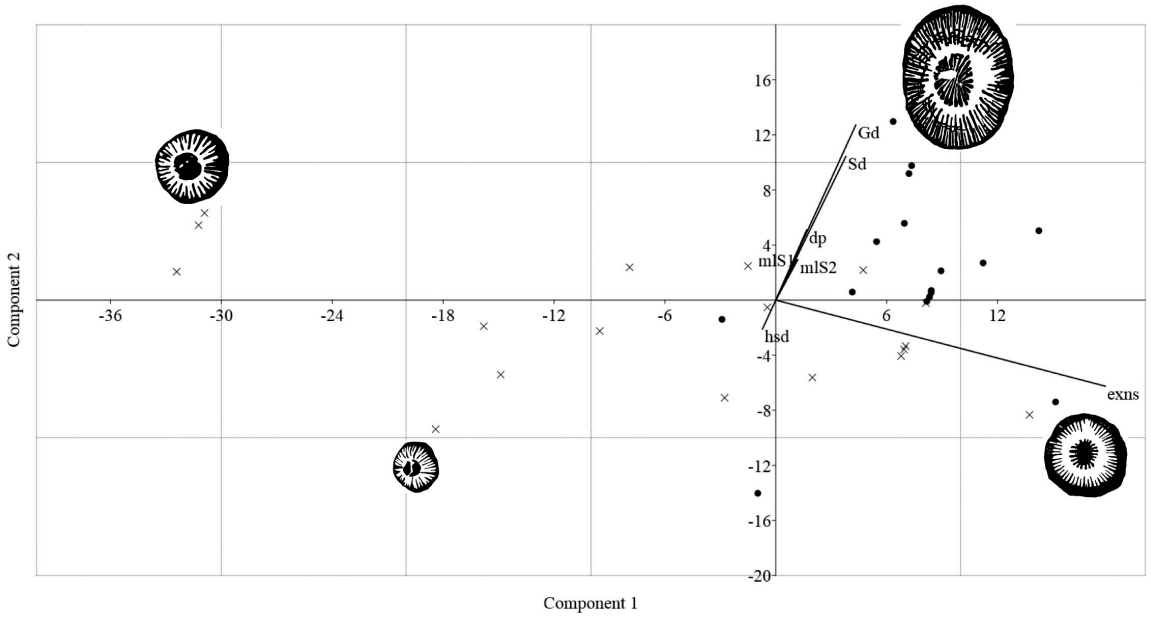


**FIGURE 10.** Set 3 PCA considering components 1 and 2, which sum gives more than 93% of variance percentage. Samples with type 1 pseudocolumella are symbolized with a dot on the graph and samples with type 2 pseudocolumella are symbolized with an "x". The influence of each character is quantified and polarized with segments. Images of coral cross sections are from the data point closest to them.

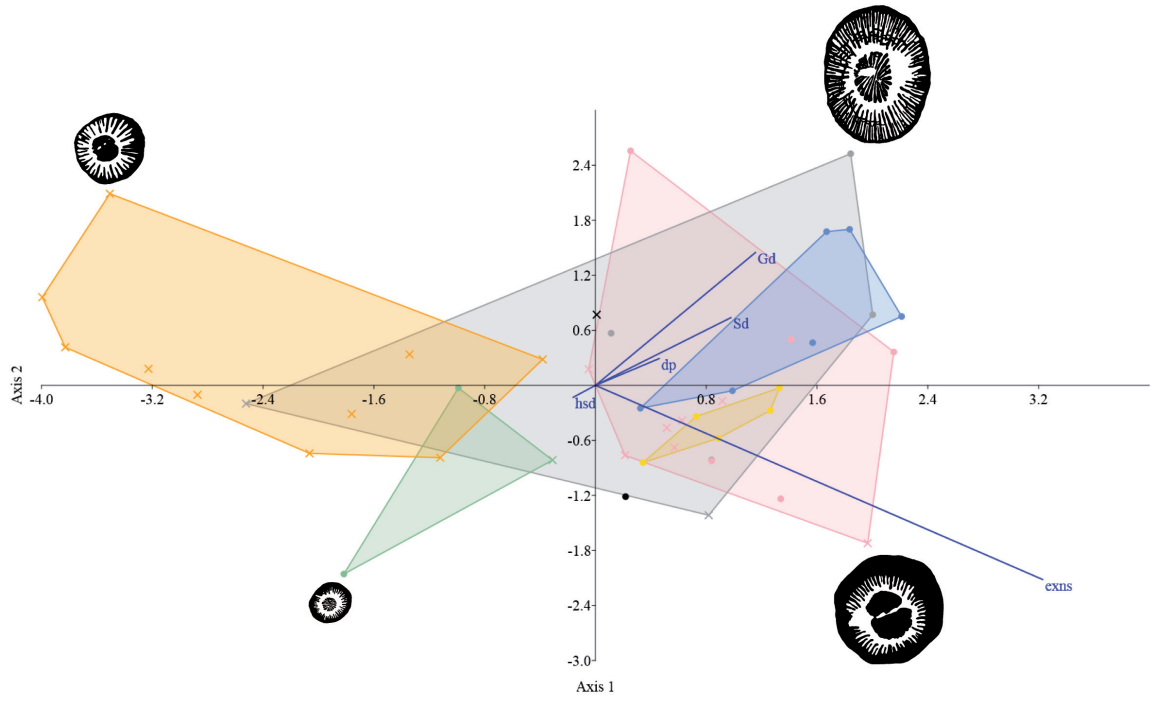


**FIGURE 11.** Set 2 discriminant analysis. Different colors correspond to different area of sampling. Pink: Amellagou olistoliths; Yellow: MNHN collections; Grey: Dades Valley; Green: Jebel Taabest; Black: Jebel Serdrar; Blue: Koudiat Ech Chehem; Orange: Taililout. Character influences are quantified and polarized with blue segments. Samples with type 1 pseudocolumella are symbolized with a dot on the graph and samples with type 2 pseudocolumella are symbolized with an "x". Images of coral cross sections are from the data point closest to them.

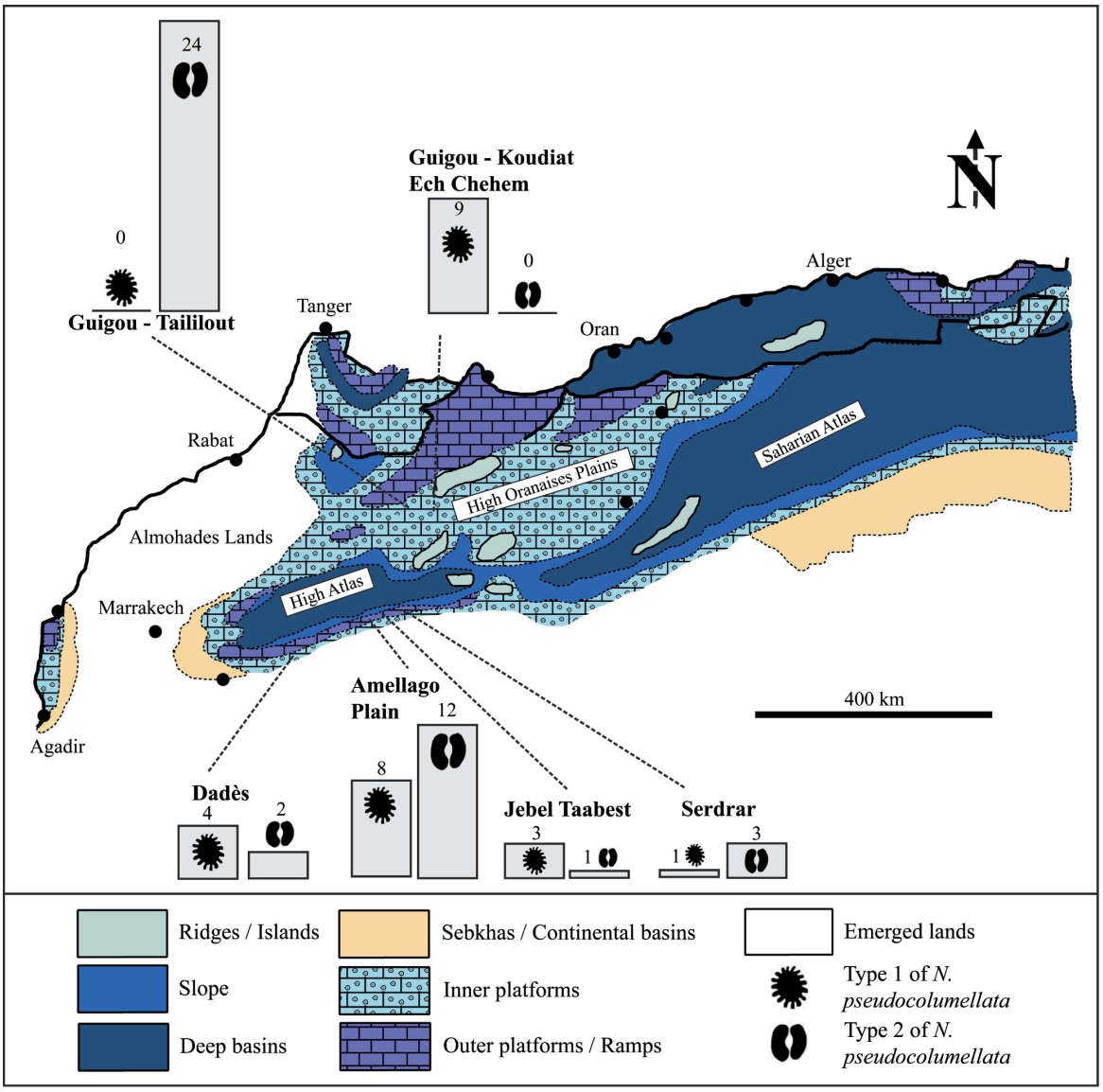


**FIGURE 12.** Distribution of the two extreme shapes of pseudocolumella (type 1 and type 2) in each sampling sites in High and Middle Atlas in Morocco; bar height indicates the number of type 1 and type 2 specimens. Facies map for the Pliensbachian modified from Ait Addi et al. (2005).

same site are morphologically linked and the distribution of type 1 and type 2 pseudocolumella follows the same trends within a single sampling site. To avoid duplications, we choose to show only two graphic results; one from PCA on set 3 (Figure 10) and one from discriminant analysis on set 2 (Figure 11).

## DISCUSSION

Without considering the question of the pseudocolumella, univariate, and multivariate statistical analyses show significant overlap in coral dimensions and number of septa, thus we conclude that all the samples belong to a single species. Since there is a correlation between locality and morphology, it can also be concluded that this taxon is strongly influenced by its living environment and not only by the slightly different ages of the samples. Nevertheless, the variability of the pseudocolumella shape makes the case more complex. The two morphologies of pseudocolumella are associated with different trends in overall morphologies of the corallites. In fact, type 2 is preferentially associated with small calicular diameters, low numbers of septa, and high septal density, which could correspond to young development

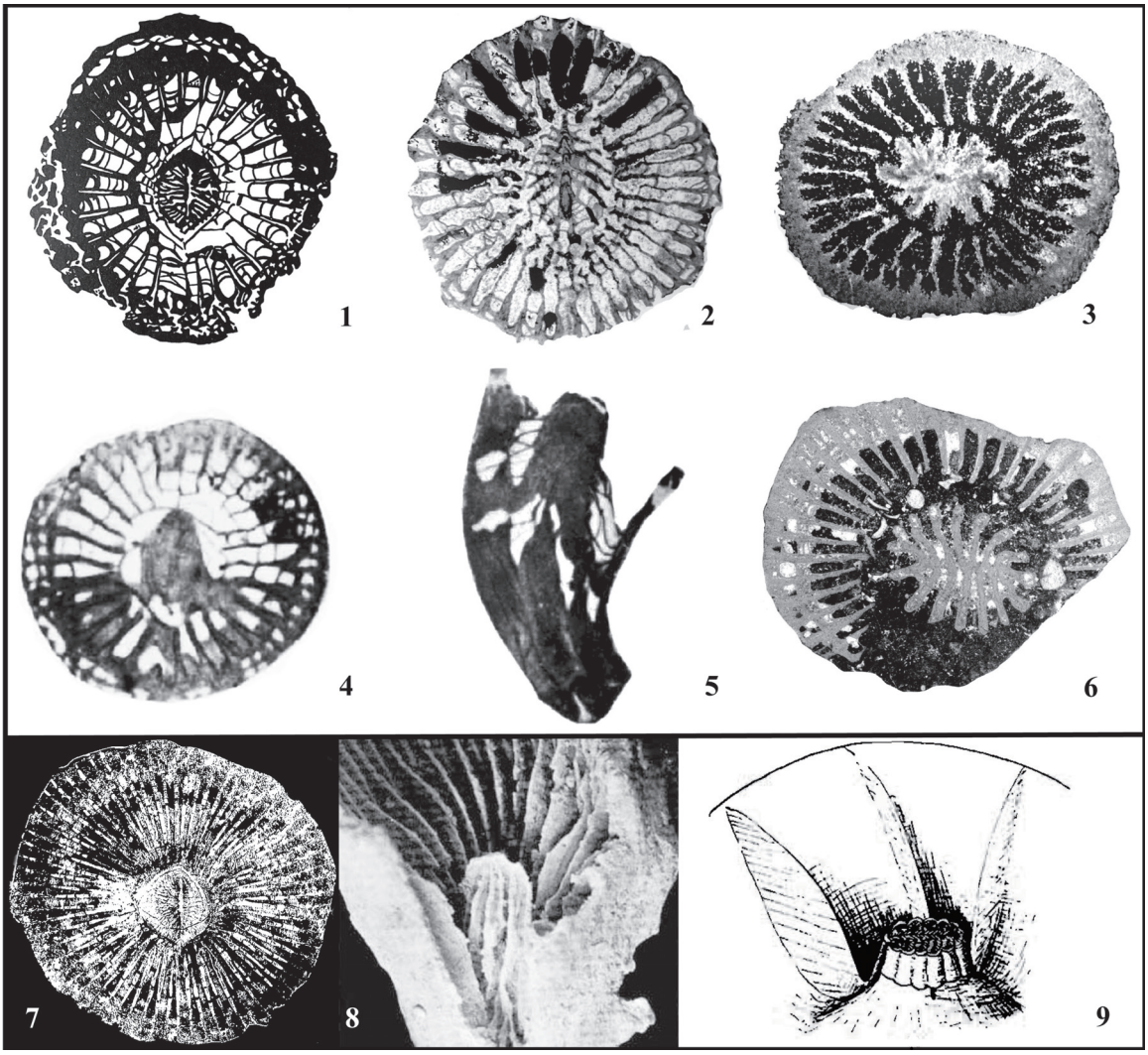


**FIGURE 13.** Comparison of *Neorylstonia pseudocolumellata* with examples of Paleozoic corals with a similar pseudocolumella axial structure. **1,** Transverse section of *Carruthersella* sp. Garwood, 1913, modified from figure 197.5a of Moore, 1956. **2,** Transverse section of *Hamaraxonia* sp. Berkowski, 2012, modified from figure 2.A of Berkowski and Weier (2012). **3,** Transverse section of *Sloveniaxon* sp. Kossovaya, 2012, modified from figure 3.B3 of Kossovaya et al. (2012). **4,** Transverse section of *Rylstonia benecompacta*, Hudson and Platt, 1927, modified from figure 234.2c of Hill (1981). **5,** Longitudinal section of *Rylstonia benecompacta*, Hudson and Platt, 1927, modified from figure 234.2d of Hill (1981). **6,** Transverse section in *Neorylstonia pseudocolumellata* (for comparison), sample AM175. **7,** Transverse section of *Amygdalophyllum sudeticum* modified from figure 3.5 of Żołyński (2000). **8,** Lateral view of the columella in a broken coral from the genus *Lophophyllidium* Grabau, 1928 modified from plate 60, figure 7 of Fedorowski (1974). **9,** Reconstruction of the axial structure in the family Amygdalophyllidae: pseudocolumella with a multilamellar structure with primary lamella marked in the axial part, septal lamellae are an integral part of columella, tabella reaching the pseudocolumella in the same manner as septum, modified from figure 4.B of Fedorowski (1970).

stages. On the other hand, type 1 is more often associated with greater calicular diameters, a higher number of septa, and smaller septal density. This can be attributed to an older or more mature development stage. In addition, the distribution of pseudocolumella morphologies in one population of corals is obviously strongly linked with the sampling area of this population (Figure 11). Taililout and Koudiat Ech Chehem populations show two extreme situations with all samples exhibiting the same pseudocolumella type (see Figure 12); thus excluding the possibility of a random sampling effect in the distributions. If there is an equal chance of sampling either pseudocolumella morphology (i.e., a 50/50 chance of sampling type 1 or type 2), the probability of observing exclusively one

pseudocolumella type in a *Neorylstonia* population (e.g., the Taililout population) would be extremely low; i.e., 24 examples of one type = $(1/2)^{24}$= 0.6 x $10^{-7}$. These unequal distributions from one outcrop to the other can be explained by three hypotheses: the type of pseudocolumella is the only difference between two distinct species within the genus *Neorylstonia*; the change in the type of pseudocolumella is the result of an evolutionary novelty among one single species and the different stratigraphic positions explain the different distributions or the type of pseudocolumella is constrained by the paleoecological conditions occurring during the life of the animals.

As Koudiat Ech Chehem is stratigraphically above Taililout, it is possible that the appearance of a type 1 pseudocolumella could be interpreted as an evolutionary novelty appearing at the end of the ontogeny in more recent *Neorylstonia*. That said, other outcrops reveal that there is no consistency in the temporal distribution of the pseudocolumella types; for example, the Choucht Formation in the Dades Valley belongs to the uppermost Domerian and includes both type 1 and 2 pseudocolumellae. The first and second hypotheses are rejected due to the coexistence of both morphologies in the same localities and even within a single sample (see Appendix 2, sample A57331-1). The co-occurrences of both morphologies in one outcrop, together with the results from univariate analysis, suggest that the type 2 pseudocolumella corresponds to a younger growth stage than the type 1.

The third hypothesis proposed is the preferred explanation for the data presented here, but the succession of the two morphologies in one single sample must be explained. As the type 1 morphology seems to be a facultative mature stage constrained by paleoecological conditions, we propose that, as a secondary character, the type 1 pseudocolumella is a mature morphology linked to sexual reproduction. This explanation would require that the type 1 shape could be associated with gonadic fixation/activity when the environment is favorable for sexual reproduction. This would imply that unfavorable conditions for sexual reproduction would lead to asexual reproduction or the total lack of breeding activity, associated with type 2 morphology. This last hypothesis is supported by the lack of budding scars on the corals, which implies that budding was restricted to the soft parts of the animals or was totally absent. Unfortunately, due to the lack of studies about the relationship between present-day coral skeletons and sexual maturity, we cannot confirm this idea with a modern coral as an analogous example. In addition, direct field observations provide no evidence of the precise ecological factors impacting *Neorylstonia pseudocolumellata* morphology.

The mode of pseudocolumella growth in *Neorylstonia* is analogous to that observed in the Rugosa subfamily Amygdalophyllinae described in Fedorowski (1970) and Żołyński (2000) (Figure 13). Another rugose coral with analogous features for the axial structure corresponds to the genus *Lophophyllidium* sensu Fedorowski (1974), which can present a lamello-tabellar pseudocolumella made of septal lamellae sustained at their base by axial tabellae. These alternations are interpreted by the author as changes in the rhythm of the secretion of the structural elements. In *Lophophyllidium*, the pseudocolumella is wrapped into concentric endothecal layers in continuity with the tabulae of the lumen (see Fedorowski, 1974) and, like *Neorylstonia,* shows a sustained increase of the axial structure when the calix does not grow anymore.

The *Neorylstonia* pseudocollumella axial structure is totally unique among Mesozoic corals. Despite a throrough literature search, no similar features could be found in Cenozoic or present-day corals either. Axial structures in post-Paleozoic corals are equally from a septal and/or endothecal origin, but the organization in septal lamellae, the bilateral symmetry, the ontogenic variations, the axial porosity, and the overcalicular apical growth found in *Neorylstonia* are singular characters that are only known in rugose corals. Type 1 and type 2 pseudocollumella are both facultative states as each can be absent in samples studied.

Another point is the question of the link between *N. pseudocolumellata* axial structure and the pseudocolumella of some rugose corals from Paleozoic (Figure 13). As phylogenetic inheritance is excluded between Paleozoic Rugosa and post-Paleozoic Scleractinia, only a convergence phenomenon can be purposed to explain the similarity of the axial structure in *N. pseudocolumellata* and some Rugosa. The affiliation of *N. pseudocolumellata* to Scleractinia is evidenced by the typical scleractinian organization of its septal apparatus in hexameral symmetry and by the probable aragonitic nature of the original skeleton (i.e., before diagenesis). Scleractinians almost exclusively biomineralize aragonitic skeletons, although rare examples of calcitic Scleractinia have been discovered (Stolarski, 2007, 2008). An original aragonitic skeleton is interpreted for *N. pseudocolumellata* because all samples collected have been inverted

to calcite (losing its initial microstructural architecture during neomorphism), whereas a calcitic coral would not be altered and thus would conserve its microstructural features. So, this similar axial organization appears to be a surprising convergence phenomenon. The key of the functional significance of this organization may be in the understanding of its ecological role in similar rugose corals. In Rugosans it is either interpreted as a structure associated with sexual reproduction (Poty, 1981) because of its development (seasonally or environmentally influenced), or as a reinforcement structure for the skeleton (Poty, personal communication, 2017). More generally, the increase of calcification associated with the formation of the pseudocolumella can be interpreted as a way to eliminate calcium carbonate ($CaCO_3$) excess in the body tissues resulting from photosynthetic activity, or also as a way to manage hypoxia (see Wooldridge, 2013 concerning general processes of calcification). In this study, we also proposed the possibility that the pseudocolumella was used to help soft tissues lift up during the growth of the septal apparatus.

## CONCLUSION

*Neorylstonia pseudocolumellata* is a small solitary Moroccan coral that lived nearshore in the far end of a western Tethyan Gulf during the late Sinemurian and Pliensbachian stages. This scleractinian coral disappeared at the Pliensbachian/Toarcian boundary. Its skeletal structure is reminiscent of the pseudocolumella structure found in some rugose corals. In Rugosa, the pseudocolumella occasionally exhibits a seasonal or environmentally-dependent development. This comparable organization results in a convergence phenomenon between some Paleozoic rugosa made of calcite and this originally aragonitic scleractinian coral. Concerning *N. pseudocolumellata*, the pseudocolumella axial structure shows two main different morphologies between the different samples and vertically within a single sample (transition stages observed). One of these morphologies (type 1) is associated with an advanced degree of maturity; it is always observed as a final stage when present, is sometimes present since the beginning of the pseudocolumella formation, but can also be absent. This environmentally-dependent type 1 morphology is proposed to be linked to sexual reproduction, possibly as a gonads-fixation structure. The type 2 morphology would thus be conditioned by the conformation of the soft tissues at the base of the polyp, in this case more relaxed and pleated. This conformation would correspond to unfavorable environmental conditions for sexual reproduction. Despite important variability in dimensions and number of septa and septal lamellae among the samples, statistical analyses do not distinguish two different species under the genus *Neorylstonia*. Due to the large variability in dimensions as well as the ontogenic modifications of the axial structure, *N. pseudocolumellata* appears to be a significant example of the possible intraspecific variability in scleractinian coral species and a unique case of true pseudocolumella in Scleractinia.

## ACKNOWLEDGMENTS

We would like to thank S. Charbonnier and J. Pacaud for their help in the collections of MNHN. Our field campaign in Middle Atlas has been successfully leaded by A. Charrière and H. El Arabi, we express our profound appreciation for that. We are equally grateful to M. Ousri and his family for the hospitality and help in the field in Morocco. We express gratitude to our friend and colleague R. Martini for her collaboration in this work and also to P. Neige and C. Meister for their precious help with the ammonite identifications. J. Sterpenich and C. Morlot are thanked for carrying out CT-Scan analysis. R. Vasseur would like to acknowledge A. Flammang and J. Moine from the laboratory of lithopreparation of Georessources, as well as C. Delangle and the association Terrae Genesis for their help in the production of thin sections. R. Martindale thanks the University of Texas at Austin for a 2015 Jackson School of Geosciences seed grant, which funded the travel associated with this work. We also would like to thank our anonymous rewievers for the wise advices that significantly enhanced the quality of this article.

## REFERENCES


Ait Addi, A., Benshili, K., Benzaggagh, M., Chafiki, D., El Hariri, K., Elmi, S., Fedan, B., Ibhou, H., and Sadki, D. 2005. *Le Jurassique Marocain: Transversale du Rif à la Bordure Saharienne, Livret Guide d'excursion du Groupe Français d'Etude du Jurassique.* Groupe Français d'Etude du Jurassique (publisher's locality unknown).

Barrois, C. 1889. Faune du Calcaire d'Erbray (Loire Inférieure). *Mémoires de la Société Géologique du Nord*, 3:1-348.

Barrois, C. 1898. Des relations des mers dévoniennes de Bretagne avec celles des Ardennes. *Annales de la Société Géologique du Nord*, 27:231-259.

Beauvais, L. 1986. Monographie des madréporaires du Jurassique inférieur du Maroc. *Palaeontographica, Abteilung A*, 194(1/3):1-68.

Berkowski, B. and Weyer, D. 2012. *Hamaraxonia*, a new pseudocolumellate genus of Middle Devonian deep-water Rugosa (Anthozoa) from Morocco. *Geologica Belgica*, 15(4):245-253.

Bodin, S., Krencker, F.-N., Kothe, T., Hoffmann, R., Mattioli, E., Heimhofer, U., and Kabiri, L. 2016. Perturbation of the carbon cycle during the late Pliensbachian – Early Toarcian: New insight from high-resolution carbon isotope records in Morocco. *Journal of African Earth Sciences*, 116:89-104. https://doi.org/10.1016/j.jafrearsci.2015.12.018

Bodin, S., Mattioli, E., Fröhlich, S., Marshall, J.D., Boutib, L., Lahsini, S., and Redfern, J. 2010. Toarcian carbon isotope shifts and nutrient changes from the Northern margin of Gondwana (High Atlas, Morocco, Jurassic): Palaeoenvironmental implications. *Palaeogeography, Palaeoclimatology, Palaeoecology*, 297:377-390. https://doi.org/10.1016/j.palaeo.2010.08.018

Bourne, G.C. 1900. The Anthozoa, p. 1-84. In Ray Lankester, E. (ed.), *A Treatise on Zoology. The Porifera and Coelentera*. Adam & Charles Black, London. https://doi.org/10.5962/bhl.title.11637

Brahmi,C., Kopp, C., Domart-Coulon, I., Stolarski, J., and Meibom, A. 2012. Skeletal growth dynamics linked to trace-element composition in the scleractinian coral *Pocillopora damicornis*. *Geochimica et Cosmochimica Acta,* 99:146-158. https://doi.org/10.1016/j.gca.2012.09.031

Burgess, S.D., Bowring, S.A., Fleming, T.H., and Elliot, D.H. 2015. High-precision geochronology links the Ferrar large igneous province with early-Jurassic ocean anoxia and biotic crisis. *Earth and Planetary Science Letters*, 415:90-99. https://doi.org/10.1016/j.epsl.2015.01.037

Caruthers, A.H., Smith, P.L., and Gröcke, D.R. 2013. The Pliensbachian–Toarcian (Early Jurassic) extinction, a global multi-phased event. *Palaeogeography, Palaeoclimatology, Palaeoecology,* 386:104-118. https://doi.org/10.1016/j.palaeo.2013.05.010

Caruthers, A.H., Smith, P.L., and Gröcke, D.R. 2014. The Pliensbachian–Toarcian (Early Jurassic) extinction: A North American perspective. *Geological Society of America Special Papers*, 505:225-243. https://doi.org/10.1130/2014.2505(11)

Caswell, B.A., Coe, A.L., and Cohen, A.S. 2009. New range data for marine invertebrate species across the early Toarcian (Early Jurassic) mass extinction. *Journal of the Geological Society*, 166:859-872. https://doi.org/10.1144/0016-76492008-0831

Charrière, A., Ibouh, H., and Haddoumi, H. 2011. The Central High Atlas from Beni Mellal to Imilchil. *Notes et Mémoires du Service Géologique du Maroc*, 559(4):1-168.

Chevalier, J.-P. 1987. Ordre des scléractiniaires, p. 403-764. In Grassé, P.P. (ed.), *Traité de Zoologie*. Masson, Paris.

Colo, G. 1961. Contribution à l'étude du Jurassique du Moyen Atlas septentrional. *Notes et Mémoires du Service Géologique du Maroc*, 139:1-226.

Cuif, J.P. 1974. Recherches sur les madréporaires du Trias. II. Astraeoidea. Révision des genres *Montlivaltia* et *Thecosmilia*. Etude de quelques types structuraux du Trias de Turquie. *Bulletin du Muséum National d'Histoire Naturelle de Paris*, 275(40):293-400.

Dana, J.D. 1846. Genera of fossil corals of the family Cyathophyllidae. *American Journal of Science*, 1:181-184.

Danise, S., Twitchett, R.J., and Little, C.T.S. 2015. Environmental controls on Jurassic marine ecosystems during global warming. *Geology*, 43:263-266. https://doi.org/10.1130/G36390.1

Danise, S., Twitchett, R.J., Little, C.T.S., and Clémence, M.-E. 2013. The impact of global warming and anoxia on marine benthic community dynamics: An example from the Toarcian (Early Jurassic). *PLoS ONE*, 8(2):1-14. https://doi.org/10.1371/journal.pone.0056255

Dera, G., Neige, P., Dommergues, J.-L., Fara, E., Laffont, R., and Pellenard, P. 2010. High-resolution dynamics of Early Jurassic marine extinctions: The case of Pliensbachian–Toarcian ammonites (Cephalopoda). *Journal of Geological Society of London*, 167:21-33. https://doi.org/10.1144/0016-76492009-068

Dommergues, J.-L. and Meister, C. 2017. Ammonites du Jurassique inférieur (Hettangien, Sinémurien, Pliensbachien) d'Afrique du Nord (Algérie, Maroc et Tunisie). Atlas d'identification des espèces. *Revue de Paléobiologie du Muséum de Genève*, 36(2):189-367.

Duncan, R., Hooper, P., Rehacek, J., Marsh, J., and Duncan, A. 1997. The timing and duration of the Karoo igneous event, southern Gondwana. *Journal of Geophysical Research*, 102:18127-18138. https://doi.org/10.1029/97JB00972

Ehrenberg, C.G. 1834. *Die corallenthiere des rothen Meeres physiologisch untersucht und systematisch verzeichnet. Beiträge zur physiologischen Kenntniss der Korallenthiere im allgemeinen, und besonders des rothen Meeres*. Physicalische abhanblungen der königlischen Akademie der Wissenschaften zu Berlin, Berlin.

El Arabi, H., Canerot, J., and Charrière, A. 1987. Dynamique récifale et tectonique distensive en blocs basculés: L'exemple des récifs liasiques du bloc du Guigou (Causse moyen atlasique-Maroc). *Archives des Sciences de la Société de Physique et d'Histoire Naturelle de Genève*, 40(3):259-271.

Ettaki, M., Chellai, E.H., Milhi, A., Sadki, D., and Boudchiche, L. 2000. Le passage Lias moyen-Lias supérieur dans la région de Todrha-Dades: événements bio-sédimentaires et géodynamiques (Haut Atlas central, Maroc). *Comptes Rendus de l'Academie des Sciences, Series IIA, Earth and Planetary Science*, 331(10):667-674. https://doi.org/10.1016/S1251-8050(00)01458-0

Fedorowski, J. 1970. Some Upper Viséan columnate tetracorals from the Holy Cross Mountains (Poland). *Acta Palaeontologica Polonica*, 15(4):549-640.

Fedorowski, J. 1974. The Upper Palaeozoic tetracoral genera *Lophophyllidium* and *Timorphyllum*. *Palaeontology*, 17(3):441-473.

Fedorowski, J. 1997. Rugosa and Scleractinia – A commentary on some methods of phylogenetic reconstructions. *Acta Palaeontologica Polonica*, 42(3):446-456.

Garwood, E.J. 1913. The Lower Carboniferous succession in the north-west of England. *Quarterly Journal of the Geological Society of London*, 68:449-586.

Goričan, Š., Carter, E.S., Guex, J., O'Dogherty, L., De Wever, P., Dumitrica, P., Hori, R.S., Matsuoka, A., and Whalen, P.A. 2013. Evolutionary patterns and palaeobiogeography of Pliensbachian and Toarcian (Early Jurassic) Radiolaria. *Palaeogeography, Palaeoclimatology, Palaeoecology*, 386:620-636. https://doi.org/10.1016/j.palaeo.2013.06.028

Guex, J., Bartolini, A., Spangenberg, J., Vicente, J.-C., and Schaltegger, U. 2012. Ammonoid multi-extinction crises during the Late Pliensbachian-Toarcian and carbon cycle instabilities. *Solid Earth Discussions*, 4:1205-1228. https://doi.org/10.5194/sed-4-1205-2012

Haeckel, E.H.P.A. 1866. *Generelle Morphologie der Organismen. Allgemeine Grundzüge der Organischen Formen-wissenschaft, Mechanisch Begründet Durch die von Charles Darwin Reformirte Descendenztheorie. Zweiter Band: Allgemeine Entwicklungsgeschichte der Organismen.* Verlag von Georg Reimer, Berlin. https://doi.org/10.5962/bhl.title.3953

Hahn, F. 1911. Neue Funde in nordalpinen Lias der Achenseagegend und bei Ehrwald. *Neues Jahrbuch für Mineralogie Geologie und Paläontologie, Beilage Band*, 32:537-557.

Hammer, Ø., Harper, D.A.T., and Ryan, P.D. 2001. PAST: Paleontological statistics software package for education and data analysis. *Palaeontologia Electronica*, 4.1.4:1-9. https://palaeo-electronica.org/2001_1/past/issue1_01.htm

Harries, P.J. and Little, C.T.S. 1999. The early Toarcian (early Jurassic) and the Cenomanian-Turonian (Late Cretaceous) mass extinction: Similarities and contrasts. *Palaeogeography Palaeoclimatology Palaeoecology*, 154:39-66. https://doi.org/10.1016/S0031-0182(99)00086-3

Hill, D. 1981. *Treatise on Invertebrate Paleontology, Part F, Coelenterata Suppl. I. Rugosa and Tabulata*. Geological Society of America and University of Kansas Press, Boulder, Colorado, and Lawrence, Kansas. https://doi.org/10.17161/dt.v0i0.5501

Hudson, R.G.S and Platt, M.I. 1927. On the Lower Carboniferous corals: The development of *Rylstonia benecompacta*, gen. et. sp. n. *Annals and Magazine of Natural History*, 19(109):39-48. https://doi.org/10.1080/00222932708633571

Jenkyns, H.C. 1985. The Early Toarcian and Cenomanian-Turonian anoxic events in Europe: Comparisons and contrasts. *International Journal of Earth Sciences (Geologische Rundschau)*, 74(3):505-518. https://doi.org/10.1007/BF01821208

Jenkyns, H.C. 1988. The early Toarcian (Jurassic) anoxic event: Stratigraphic, sedimentary and geochemical evidence. *American Journal of Science*, 288:101-151. https://doi.org/10.2475/ajs.288.2.101

Jenkyns, H.C. 2003. Evidence for rapid climate change in the Mesozoic-Palaeogene greenhouse world. *Philosophical Transactions of the Royal Society A: Mathematical, Physical and Engineering Sciences*, 361:1885-1916. https://doi.org/10.1098/rsta.2003.1240

Jenkyns, H.C. and Clayton, C.J. 1986. Black shales and carbon isotopes in pelagic sediments from the Tethyan Lower Jurassic. *Sedimentology*, 33:87-106. https://doi.org/10.1111/j.1365-3091.1986.tb00746.x

Kossovaya, O.L., Nowak, M., and Weyer, D. 2012. *Sloveniaxon*, a new genus of ahermatypic Rugosa (Anthozoa) from the basal Permian (Asselian) of Slovenia. *Geologica Belgica*, 15(4):361-369.

Lachkar, N., Guiraud, M., Harfi, A.E., Dommergues, J.-L., Dera, G., and Durlet, C. 2009. Early Jurassic normal faulting in a carbonate extensional basin: Characterization of tectonically driven platform drowning (High Atlas rift, Morocco). *Journal of the Geological Society*, 166:413-430. https://doi.org/10.1144/0016-76492008-084

Lathuilière, B. and Marchal, D. 2009. Extinction, survival and recovery of corals from the Triassic to Middle Jurassic Time. *Terra Nova*, 21:57-66. https://doi.org/10.1111/j.1365-3121.2008.00856.x

Littler, K., Hesselbo, S.P., and Jenkyns, H.C. 2010. A carbon-isotope perturbation at the Pliensbachian–Toarcian boundary: Evidence from the Lias Group, NE England. *Geological Magazine*, 147(2):181-192. https://doi.org/10.1017/S0016756809990458

Martindale, R.C. and Aberhan, M. 2017, Response of macrobenthic communities to the Toarcian Oceanic Anoxic Event in northeastern Panthalassa (Ya Ha Tinda, Alberta, Canada): *Palaeogeography, Palaeoclimatology, Palaeoecology*, 478:103-120. https://doi.org/10.1016/j.palaeo.2017.01.009

Mattioli, E., Plancq, J., Boussaha, M., Duarte, L.V., and Pittet, B. 2013. Calcareous nannofossil biostratigraphy: New data from the Lower Jurassic of the Lusitanian Basin. *Comunicaçõe Geológicas*, 100(I):69-76.

Melnikova, G.K. 1974. Osobennosti gistologicheskikh struktur i mikrostruktur septalnogo aparata u pozdnetriasovykh skleraktinii. *Trudy (Institut geologii i geofiziki. Sibirskoe Otdelenie),* 201:224-228.

Melnikova, G.K. 1975. Novye rannejurskie predstaviteli Amphiastraeina (Skleraktinii) jugo-vostocnogo Pamira, p. 108-120. In Dzalilov, V. (ed.), *Voprocy Paleontologii Tadjikistana.* Akademija Nauk Tadzikskoj SSR, Dushanbe.

Milne Edwards, H. and Haime, J. 1848. Recherches sur les polypiers. Mémoire 1. Observations sur la structure et le development des polypiers en general. *Annales des Sciences Naturelles*, *Zoologie,* 9(4):37-89.

Milne Edwards, H. and Haime, J. 1854. *A Monograph of the British Fossil Corals*. Paleontographical Society, London. https://doi.org/10.5962/bhl.title.11691

Moore, R.C. 1956. *Treatise on Invertebrate Paleontology*. Geological Society of America and University of Kansas Press, Boulder, Colorado, and Lawrence, Kansas.

Morabet, A. 1974. *The Lias Reefs of the Middle Atlas Platform, Morocco*. Unpublished Master of Science Thesis, University of South Carolina, Columbia, South Carolina, USA.

Morard, A., Guex, J., Bartolini, A., Morettini, E., and De Wever, P. 2003. A new scenario for the Domerian–Toarcian transition. *Bulletin de la Société Géologique de France*, 174(4):351-356. https://doi.org/10.2113/174.4.351

Neave, S.A. 1940. *Nomenclator Zoologicus. A List of the Names of Genera and Subgenera in Zoology from the Tenth Edition of Linnaeus 1758 to the End of 1935, Vol. III*. Zoological Society of London, London.

Oliver, W.A. 1980. The relationship of the scleractinian corals to the rugose corals. *Paleobiology*, 6(2):146-160. https://doi.org/10.1017/S0094837300006709

Pálfy, J., Smith, P.L., and Mortensen, J.K. 2002. Dating the end-Triassic and Early Jurassic mass extinctions, correlative large igneous provinces, and isotopic events. *Catastrophic Events and Mass Extinctions: Impacts and Beyond. Geological Society of America Special Paper*, 356:523-532. https://doi.org/10.1130/0-8137-2356-6.523

Poty, E. 1981. Recherches sur les Tétracoralliaires et les Hétérocoralliaires du Viséen de la Belgique. *Mededelingen Rijks Geologische Dienst*, 35:1-161.

Pryvalov, V.A., Pironon, J., Izart, A., and Morlot, C. 2017. Exploration of architecture and connectivity of cleat arrays in coals of the Lorraine CBM play by the means of X- ray computer tomography. *79th EAGE Conference and Exhibition 2017,* Paris, p. 1388-1392. https://doi.org/10.3997/2214-4609.201700758

Raup, D.M. and Sepkoski, J.J. 1984. Periodicity of extinctions in the geologic past. *Proceedings of the National Academy of Sciences*, 81:801-805. https://doi.org/10.1073/pnas.81.3.801

Raup, D.M. and Sepkoski, J.J. 1986. Periodic extinction of families and genera. *Science*, 231:833-836. https://doi.org/10.1126/science.11542060

Röhl, H.-J., Schmid-Röhl, A., and Oschmann, W. 2001. The Posidonia Shale (Lower Toarcian) of SW-Germany: An oxygen-depleted ecosystem controlled by sea level and palaeoclimate. *Palaeogeography, Palaeoclimatology, Palaeoecology*, 165:27-52. https://doi.org/10.1016/s0031-0182(00)00152-8

Rosales, I., Quesada, S., and Robles, S. 2004. Paleotemperature variations of Early Jurassic seawater recorded in geochemical trends of belemnites from the Basque–Cantabrian basin, northern Spain. *Palaeogeography, Palaeoclimatology, Palaeoecology*, 203:253-275. https://doi.org/10.1016/S0031-0182(03)00686-2

Sarih, S. 2008. *Geodynamique et Transferts Sédimentaires Gravitaires des Bassins Liasiques du Haut-Atlas Central (Maroc).* Unpublished PhD Thesis, Université de Bourgogne, Dijon, France.

Schlüter, C. 1889. Anthozoen des reinischen Mittel-Devon. *Abhandlungen zur geologischen Spezialkarte von Preussen und den Thüringischen Staaten*, 8(4):259-465.

Schmid-Röhl, A., Röhl, H.J., and Oschmann, W. 2002. Paleoenvironmental reconstruction of Lower Toarcian epicontinental black shales (Posidonia Shale, SW Germany): Global versus regional control. *Geobios*, 35:13-20. https://doi.org/10.1016/S0016-6995(02)00005-0

Sell, B., Ovtcharova, M., Guex, J., Bartolini, A., Jourdan, F., Spangenberg, J.E., Vicente, J.-C., and Schaltegger, U. 2014. Evaluating the temporal link between the Karoo LIP and climatic–biologic events of the Toarcian Stage with high-precision U–Pb geochronology. *Earth and Planetary Science Letters*, 408:48-56. https://doi.org/10.1016/j.epsl.2014.10.008

Stolarski, J. 2003. Three-dimensional micro- and nanostructural characteristics of the scleractinian coral skeleton: A biocalcification proxy. *Acta Palaeontologica Polonica*, 48(4):497-530.

Stolarski, J., Meibom, A., Przenioslo, R., and Mazur, M. 2007. A Cretaceous Scleractinian coral with a calcitic skeleton. *Science*, 318:92-94. https://doi.org/10.1126/science.1149237

Stolarski, J., Meibom, A., Mazur, M., and Phillips, G.E. 2008. Calcitic Scleractinian corals: When, where and why? *2008 Joint Meeting of The Geological Society of America, Soil Science Society of America, American Society of Agronomy, Crop Science Society of America, Gulf Coast Association of Geological Societies with the Gulf Coast Section of SEPM*, the Geological Society of America, Houston, p. 201.

Suan, G., Mattioli, E., Pittet, B., Lécuyer, C., Suchéras-Marx, B., Duarte, L.V., Philippe, M., Reggiani, L., and Martineau, F. 2010. Secular environmental precursors to Early Toarcian (Jurassic) extreme climate changes. *Earth and Planetary Science Letters*, 290(3-4):448-458. https://doi.org/10.1016/j.epsl.2009.12.047

Trecalli, A., Spangenberg, J., Adatte, T., Föllmi, K.B., and Parente, M. 2012. Carbonate platform evidence of ocean acidification at the onset of the early Toarcian oceanic anoxic event. *Earth and Planetary Science Letters*, 357-358:214-225. https://doi.org/10.1016/j.epsl.2012.09.043

Vakhrameyev, V.A. 1982. *Classopollis* pollen as an indicator of Jurassic and Cretaceous climate. *International Geology Review*, 24(10):1190-1196. https://doi.org/10.1080/00206818209451058

Vaughan, T.W. and Wells, J.W. 1943. *Revision of the Suborders, Families, and Genera of the Scleractinia*. Geological Society of America, New York. https://doi.org/10.1130/SPE44

Verrill, A.E. 1865. Classification of polyps. (Extract condensed from a synopsis of the Polypi of the North Pacific exploring expedition under Captains Ringgold and Rodgers, U.S.N.). *Annals and Magazine of Natural History*, 16:191-197. https://doi.org/10.1080/00222936508679407

Vieira, C.O.C. 1942. Ensaio monográfico sobre os quirópteros do Brasil. *Arquivos de Zoologia do Estado de São Paulo*, 3:219-417.

Waterhouse, C.O. 1902. *Index Zoologicus. An Alphabetical List of Names of Genera and Subgenera Proposed for Use in Zoology as Recorded in the "Zoological Record" 1880-1900, Together with Other Names not Included in the "Nomenclator Zoologicus" of S.H. Scudder*. Zoological Society of London and Gurney and Johnson, London. https://doi.org/10.5962/bhl.title.34443

Wells, J.W. 1969. The formation of dissepiments in Zoantharian corals, p. 17-26. In Campbell, K.S.W. (ed.), *Stratigraphy and Palaeontology Essays in Honour of Dorothy Hill*. Australian University Press, Canberra.

Wooldridge, S. 2013. A new conceptual model of coral biomineralisation: Hypoxia as the physiological driver of skeletal extension. *Biogeosciences* 10:2867-2884. https://doi.org/10.5194/bg-10-2867-2013

Żołyński, L. 2000. *Amygdalophyllum sudeticum* sp. nov. (Rugosa) from a Lower Visean gneissic conglomerate, Bardzkie Mts., Sudetes (Poland). *Acta Geologica Polonica*, 50(3):335-342.

## APPENDIX 1.

Apparent shape of pseudocolumella in transverse or slightly inclined sections for different samples.

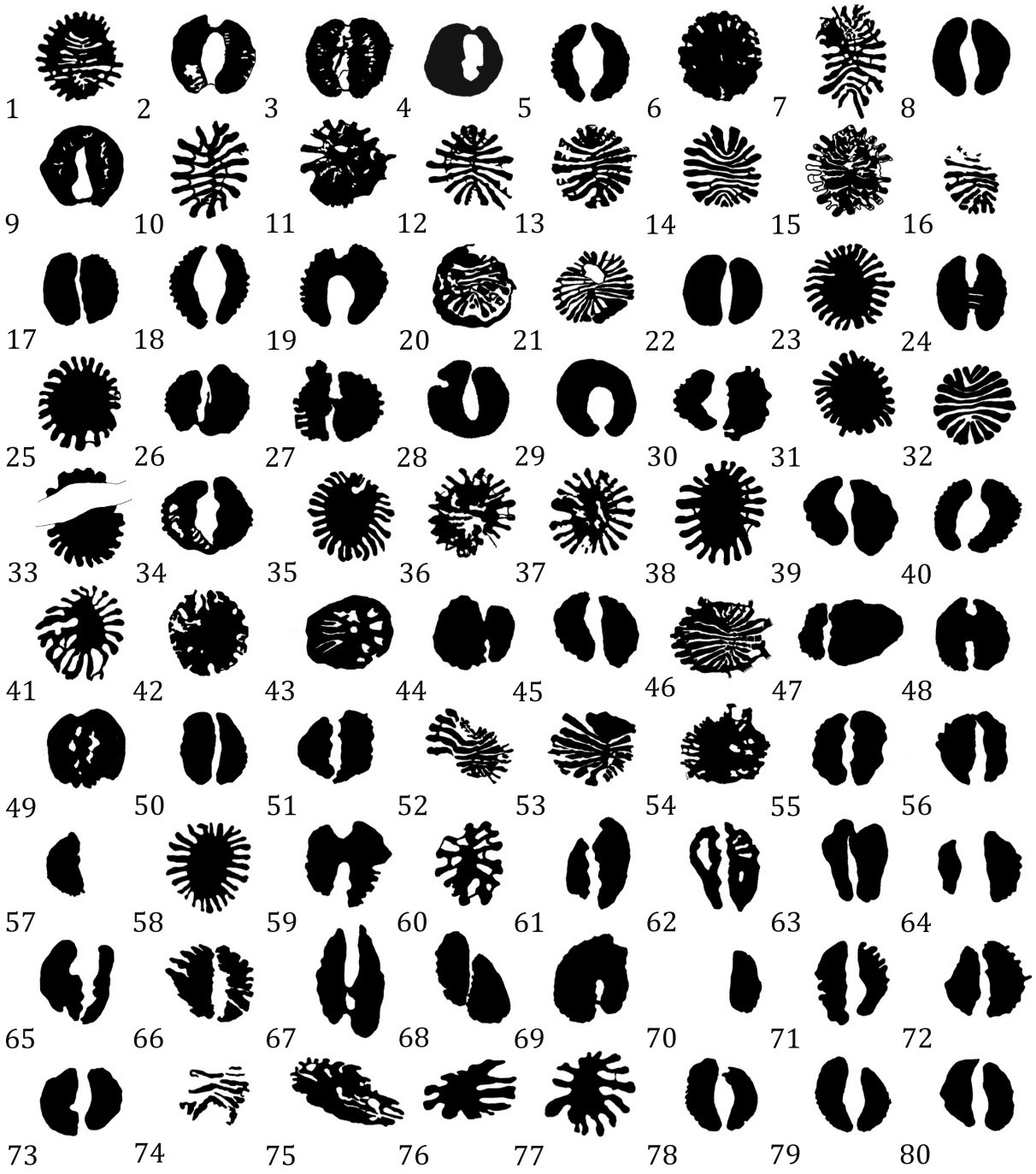

## APPENDIX 2.

X-ray transverse sections all along the sample A57331-1 provided by the nanotom S phoenix 180 kV CT-scan of Georessources laboratory in Nancy. The images are ordered following the orientation from the lowest part of the sample (in living position) to its top.

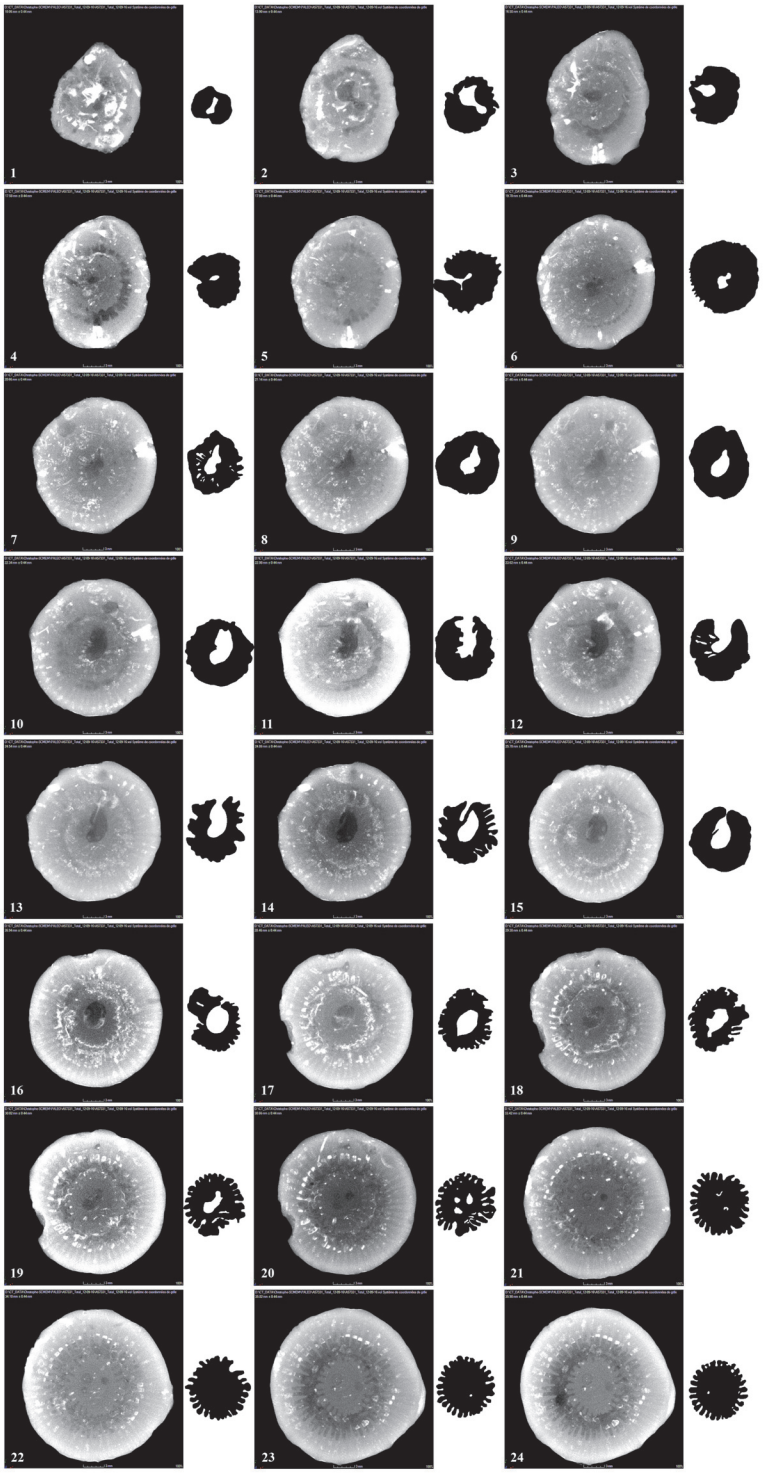

## APPENDIX 3.

X-ray transverse sections all along the sample AM16161 provided by the nanotom S phoenix 180 kV CT-scan of Georessources laboratory in Nancy. The images are ordered following the orientation from the lowest part of the sample (in living position) to its top and corresponds to the exploitable part of a longer fragment of *Neorylstonia pseudocolumellata*.